Eur. Phys. J. A (2025) 61:70
https://doi.org/10.1140/epja/s10050-025-01537-1

THE EUROPEAN PHYSICAL JOURNAL A

Review

The $^{12}C(\alpha, \gamma)^{16}O$ reaction, in the laboratory and in the stars

R. J. de Boer[1,a], A. Best[2,3], C. R. Brune[4], A. Chieffi[5,6,7], C. Hebborn[8,9,10], G. Imbriani[2,3], W. P. Liu[11,12], Y. P. Shen[11], F. X. Timmes[13], M. Wiescher[1]

[1] Department of Physics and Astronomy, University of Notre Dame, Notre Dame, IN 46556, USA
[2] Dipartimento di Fisica "E. Pancini", Università degli Studi di Napoli "Federico II", Via Cintia, 80126 Naples, Italy
[3] INFN, Sezione di Napoli, Via Cintia, 80126 Naples, Italy
[4] Department of Physics and Astronomy, Ohio University, Athens, OH 45701, USA
[5] Istituto Nazionale di Astrofisica-Istituto di Astrofisica e Planetologia Spaziali, Via Fosso del Cavaliere 100, 00133 Rome, Italy
[6] Monash Centre for Astrophysics (MoCA), School of Mathematical Sciences, Monash University, Melbourne, VIC 3800, Australia
[7] INFN, Sezione di Perugia, via A. Pascoli s/n, 06125 Perugia, Italy
[8] Université Paris-Saclay, CNRS/IN2P3, IJCLab, 91405 Orsay, France
[9] Facility for Rare Isotope Beams, Michigan State University, East Lansing, MI 48824, USA
[10] Department of Physics and Astronomy, Michigan State University, East Lansing, MI 48824, USA
[11] China Institute of Atomic Energy, P.O. Box 275(10), Beijing 102413, China
[12] Department of Physics, Southern University of Science and Technology, Shenzhen 518055, China
[13] School of Earth and Space Exploration, Arizona State University, Tempe, AZ 85287, USA

Received: 20 December 2024 / Accepted: 2 March 2025

Communicated by David Blaschke

Abstract The evolutionary path of massive stars begins at helium burning. Energy production for this phase of stellar evolution is dominated by the reaction path $3\alpha \rightarrow {}^{12}C(\alpha, \gamma)^{16}O$ and also determines the ratio of $^{12}C/^{16}O$ in the stellar core. This ratio then sets the evolutionary trajectory as the star evolves towards a white dwarf, neutron star or black hole. Although the reaction rate of the 3α process is relatively well known, since it proceeds mainly through a single narrow resonance in ^{12}C, that of the $^{12}C(\alpha, \gamma)^{16}O$ reaction remains uncertain since it is the result of a more difficult to pin down, slowly-varying, portion of the cross section over a strong interference region between the high-energy tails of subthreshold resonances, the low-energy tails of higher-energy broad resonances and direct capture. Experimental measurements of this cross section require herculean efforts, since even at higher energies the cross section remains small and large background sources are often present that require the use of very sensitive experimental methods. Since the $^{12}C(\alpha, \gamma)^{16}O$ reaction has such a strong influence on many different stellar objects, it is also interesting to try to back calculate the required rate needed to match astrophysical observations. This has become increasingly tempting, as the accuracy and precision of observational data has been steadily improving. Yet, the pitfall to this approach lies in the intermediary steps of modeling, where other uncertainties needed to model a star's internal behavior remain highly uncertain.

1 Introduction

The $^{12}C(\alpha, \gamma)^{16}O$ reaction has long been the "Holy Grail" of nuclear astrophysics, determining the $^{12}C/^{16}O$ abundance ratio in our universe, the two most critical elements for the emergence of life as we know it. Wider impact studies associated with the evolution of massive stars towards supernovae, white dwarf analysis, and black hole studies suggest that the reaction has an enormous impact on a wide range of stellar environments, impacting a broad range of astrophysical observables.

The $^{12}C(\alpha, \gamma)^{16}O$ reaction, following the 3α process, is the most important reaction in stellar helium burning at temperatures of around 0.2 GK. This corresponds to a Gamow energy of about 300 keV for the average temperature regime at which the cross section is estimated to be a staggeringly small 2×10^{-17} barn. Even the most state-of-the-art measurements today fall well short of this level of sensitivity. Because the reaction cannot be measured directly at stellar energies, direct measurements are made at higher energies to establish the trend of the cross section, providing a basis for an extrapolation. Of course, to make a meaningful extrapolation, a model must be employed. To date, the most successful of these has been phenomenological R-matrix [37,63] and it has been used since the early days of experimental study of this reaction [40], although its implementation has become increasingly sophisticated.

[a] e-mail: rdeboer1@nd.edu (corresponding author)

Published online: 01 April 2025

The most recent review of the $^{12}C(\alpha, \gamma)^{16}O$ reaction by deBoer et al. [36] still relies heavily on this methodology and in particular on the use of Asymptotic Normalization Coefficients (ANCs). At that time, the use of ANCs was becoming a well established method of providing additional constraints to R-matrix analyses, providing a much more reliable and precise constraint for the particle strength of subthreshold levels over that of spectroscopic factors [75]. While there have been few additional new measurements [102] in the last few years, there have been several indirect ones that have continued to test the use of ANCs [52,76,99]. Recently, first-principle predictions of light systems have been used to improve the analysis conducted in indirect studies to evaluate relevant ANCs [52]. In addition, the more precise $^{12}C(\alpha, \gamma)^{16}O$ reaction rate presented in deBoer et al. [36] has been utilized in several astrophysical models, including those used for the calculation of the black hole mass gap and for stellar seismology, providing another interesting area of discussion for this work.

This work will review experimental nuclear physics efforts to improve the uncertainty in the $^{12}C(\alpha, \gamma)^{16}O$ cross section in Sect. 2, discuss relevant nuclear theory improvements in Sect. 3, observational constraints and astrophysics modeling in Sect. 4 and discuss ideas for paths forwards in Sect. 5.

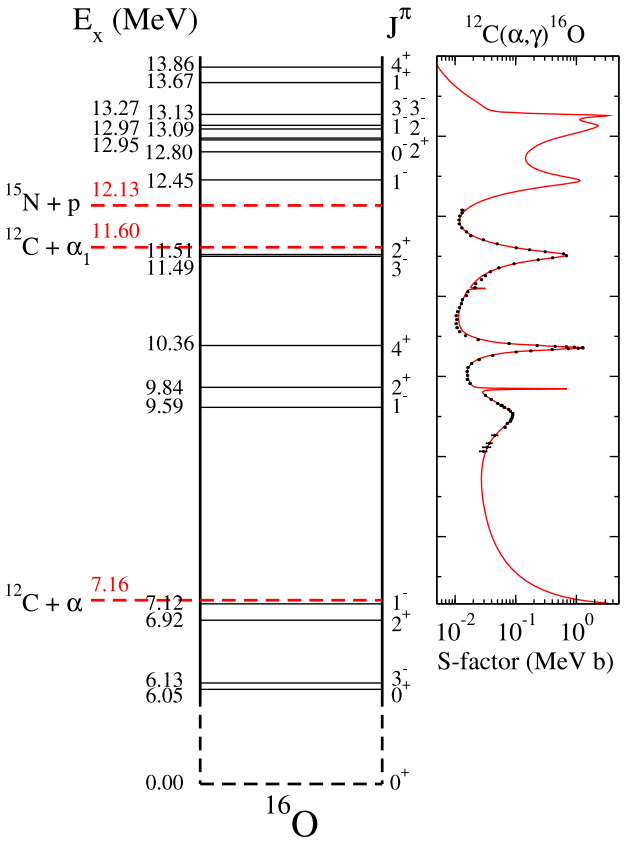

Fig. 1 Relevant level scheme of the ^{16}O system. The experimental data are those of Schürmann et al. [97] and the R-matrix calculation is from deBoer et al. [36]. Figure adapted from deBoer et al. [36]

2 New experimental nuclear physics results

Over the last decade, direct measurements of the $^{12}C(\alpha, \gamma)^{16}O$ reaction have dwindled and experimental studies have concentrated on indirect approaches. The lack of direct studies is not an indication of reduced interest in the reaction, but instead a result of improvements in indirect techniques and the difficulty of making additional direct measurements with the same techniques. In the following section these new indirect studies will be reviewed.

2.1 Primer

Before jumping into the main review of this reaction, a brief primer is given. The $^{12}C(\alpha, \gamma)^{16}O$ reaction has become so ubiquitous in the field of nuclear astrophysics that it has even developed some of its own jargon that is unique to the reaction. For instance, the reaction is often referred to by its shorthand moniker "CTAG".

At low energies, below a center-of-mass energy of about 1 MeV, the total radiative capture cross section is dominated by the ground state transition. While the other transitions, dubbed "the cascade transitions", make up less than 10% of the total. These cascade transitions consist of those passing through the other four bound states of ^{16}O (see Fig. 1) and it is a helpful circumstance that all of the secondary transitions through all of these bound states have nearly 100% branchings directly to the ground state. Thus, they can be measured nearly equivalently by detection of either the primary or secondary γ-rays in the cascade. In principle, the direct capture through these cascade transitions could be used to constrain the ANCs of the bound states, but because their cross sections are so small, this has proven to be very challenging.

Because both the α-particle and ^{12}C are spin zero particles, conservation laws result in some simplification. In particular, only natural parity states (total spin must equal angular momentum, $J = \ell$, and the parity must equal $(-1)^{\ell}$) can be populated. Finally, for the ground-state transition, the γ-ray multipolarity is limited to electric, where only $E1$ and $E2$ have been observed experimentally. Because of this, the ground state transition has historically been further subdivided into the $E1$ and $E2$ cross sections, which both make compatible contributions at low energy. While this practice is useful for understanding the important reaction components, some works have only reported these $E1$ and $E2$ cross sections instead of the actual angular distributions that were measured. This has often made it more difficult to understand discrepancies between the different measurements.

In addition, many radiative capture reactions have sizable direct capture contributions at low energy. Again, the ground

state results in a special circumstance where the effective charge term is nearly zero for $E1$ direct capture, highly suppressing it. $E2$ direct capture, by itself, is small compared to the resonance contributions, but its interference with the resonances may be strong enough to produce a significant effect.

The extrapolation of the $^{12}C(\alpha,\gamma)^{16}O$ reaction is challenging, and therefore has a large uncertainty, because the cross section over the energy region of helium burning, about 0.3 MeV, is not dominated by a single resonance but is the result of the delicate interference between the tail contributions of both subthreshold resonances and broad higher energy resonances. While the energy dependence of these broad higher-energy resonances can be measured, doing so accurately with repeatably consistent results has proven to be challenging. Further, the strength of the subthreshold states was for many years characterized by spectroscopic factors, but these suffer from a combination of experimental and theoretical uncertainties. Instead, using ANCs allows us to decrease this theory dependence (see recent review by Tribble et al. [110]), which it certainly has, but not entirely, with the smallest uncertainties being estimated to be about 10% under the most ideal of circumstances.

Phenomenological R-matrix has been the analysis tool of choice for performing these extrapolations. The ANCs of bound states can be related to reduced widths and the theory is capable of directly fitting both the radiative capture data itself and also data sets such as elastic scattering and β-delayed α-particle emission spectra. But, while versatile, phenomenological R-matrix lacks any fundamental knowledge of the nuclear potential and each resonance is included individually, where its energy, partial decay widths, and, of prime importance for the present case, relative interference signs between resonances, are only determined by comparing to experimental data.

Finally, in principle there is quite enough experimental data to well constrain the low energy cross section, but one real road block has been the lack of reproducibility between different measurements. Therefore, significant improvement can be made if a new generation of measurements are able to produce consistent results with well-defined uncertainties. It should be emphasized that these measurements shouldn't just be limited to low energies, but should focus on a consistent mapping over a wide energy range, especially in interference regions at higher energies.

2.2 Photodisintegration measurements

The only new experimental measurement of the $^{12}C(\alpha,\gamma)^{16}O$ reaction since deBoer et al. [36] is by the time-reversal reaction, the photodisintegration of ^{16}O [102], which was made at the High Intensity γ-ray source (HIγS) [117]. Measurements of $^{16}O(\gamma,\alpha)^{12}C$ may have some distinct advantages over the forward reaction. For instance, detailed balance leads to an enhancement in the cross section of ≈ 15 at 300 keV above the threshold, increasing rapidly at higher energy, reaching ≈ 70 on top of the first broad 1^- resonance at 2.25 MeV above threshold as shown in Fig. 2b. In addition, the method has completely different systematic uncertainties, including backgrounds, from the direct reaction measurement. However, there are also significant challenges. For instance, the inverse reaction only populates the ground state transition, which is mitigated in this case because this is the dominant transition at low energies. Other experimental complications include accurate γ-ray beam intensity and resolution characterization, as the γ-ray beam, while monoenergetic compared to a Bremsstrahlung beam, still has a significant energy spread and asymmetric distribution.

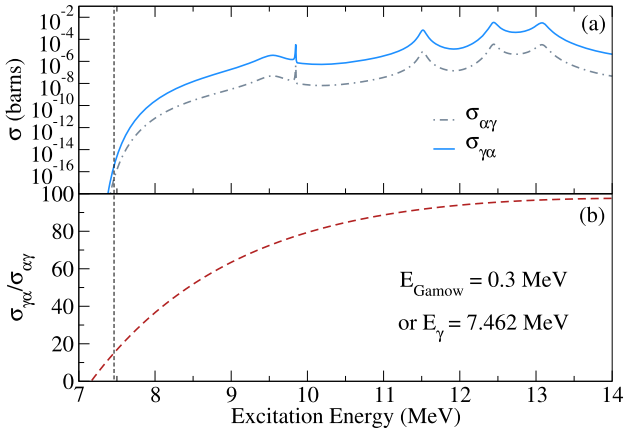

Fig. 2 (a) Comparison of the $^{12}C(\alpha,\gamma_0)^{16}O$ reaction with its inverse $^{16}O(\gamma,\alpha_0)^{12}C$ reaction. (b) Ratio of the (γ,α_0) to the (α,γ_0) cross section. The dashed line denotes the Gamow energy

Smith et al. [102] have measured the differential cross section at six energies over the energy region of the broad resonance that corresponds to the first unbound 1^- state in ^{16}O (see Fig. 4). The four angular distributions reported in that work have been compared with the R-matrix fit from deBoer et al. [36] in Fig. 3. A good reproduction of the data by the R-matrix fit is found if the data are shifted up in energy by $\approx$22 keV, which is well within the energy uncertainty of $\pm$30 keV estimated by Smith et al. [102]. While the measurements made so far only cover the higher energy range in the vicinity of the 1^- resonance, this work has demonstrated the feasibility of this technique, paving the way for future lower energy measurements using the inverse reaction.

2.3 ANC measurements

The reliance on the ANCs inferred from transfer reaction measurements resulted in a somewhat smaller estimate of the extrapolated S-factor at $E_{\mathrm{c.m.}} = 300$ keV (center-of-mass energy) by deBoer et al. [36] than most other recent ones,

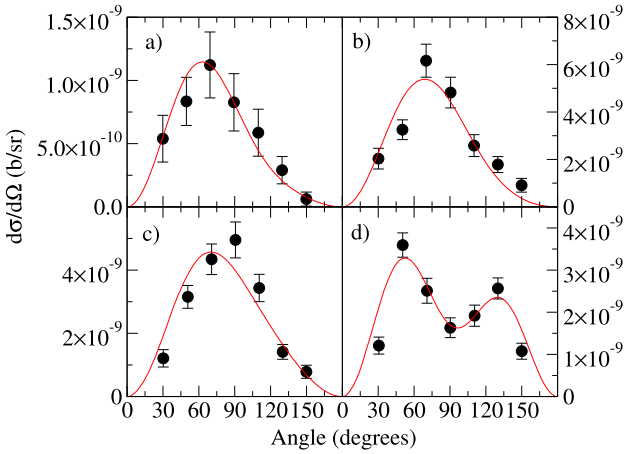

Fig. 3 Comparison of the angular distributions measured by Smith et al. [102] at $E^{\text{eff}}_{\text{c.m.}}$ = 2.02 **a**, 2.29 **b**, 2.47 **c** and 2.64 MeV **d** with the *R*-matrix fit of deBoer et al. [36]. The *R*-matrix cross section was found to be in considerably better agreement with the data if the effective energies of the data were increased by 22 keV, within the estimated uncertainty of ± 30 keV estimated in Smith et al. [102]. Since the data were presented in arbitrary units in Smith et al. [102], they have been scaled to that of the *R*-matrix cross section

giving a value of $S(300) = 140 \pm 21_{(\text{MC})}{}^{+18}_{-11(\text{model})}$ keV b. Most notably, the widely used previous rate estimate by Kunz et al. [62] had obtained $S(300) = 165(50)$ keV b when no constraints from ANCs were utilized. Yet the reason that the additional constraints from ANCs were utilized in deBoer et al. [36] was, as shown in Fig. 4, because the data from different measurements have different low energy trends that are sometimes inconsistent with one another. This is most clearly visible in the ground state $E1$ data of Kettner et al. [58], Redder et al. [89] and Gialanella et al. [50] which all trend to larger values below ≈ 2 MeV compared to the data of Dyer and Barnes [40], Kremer et al. [60], Ouellet et al. [83], Roters et al. [93], Kunz et al. [61], Fey [44], Assunção et al. [10], Makii et al. [67] and Plag et al. [86]. Similarly the $E2$ data of Redder et al. [89], Ouellet et al. [83] and Kunz et al. [61] tend to a larger value than Fey [44], Assunção et al. [10], Makii et al. [67] and Plag et al. [86]. Further, it is not just that the data have different trends, but that those that tend to the lower values are also more consistent with each other. This is not an uncommon phenomenon for low energy charged particle induced cross section data in general, where low yield measurements make discrimination between signal and background extremely challenging. A good recent example can be found in the $^{13}\text{C}(\alpha, n)^{16}\text{O}$ reaction, where the more recent measurements of Ciani et al. [33] and Gao et al. [49] show a low energy trend that increasingly deviates to smaller cross section values at low energies compared to that of Drotleff et al. [38].

The uncertainties in the extraction of the relevant partial widths are now dominated by the experimental errors and the theoretical model used to describe the transfer reaction. In particular, the choice of the reaction model and the interactions inputted in these models directly impact the normalization of the transfer cross sections and hence the extracted ANCs. Recently, Hebborn et al. [52] have reanalyzed $^{12}\text{C}(^6\text{Li}, d)^{16}\text{O}$ transfer data [11,25] constraining the ^{6}Li wavefunction with a first-principle calculation [51]. They extracted ^{12}C-α ANCs-squared of ^{16}O bound states that are 22% smaller compared to the original analyses [11,25]. Within this context, Hebborn et al. [52] have also pointed out several sources of uncertainties in the analysis of transfer reactions, and some developments in reaction theory that should be conducted to improve the analysis of α-particle transfer data.

New α-particle ANC measurements have focused primarily on using different types of transfer reactions, as opposed to the traditional (^{6}Li, d) and (^{7}Li, t) reactions. For instance, in Nan et al. [77], Shen et al. [99], and Shen et al. [100], the ANCs of the 2^+, 1^- and 0^+ (ground state) were each investigated using the $^{12}\text{C}(^{11}\text{B}, ^7\text{Li})^{16}\text{O}$ reaction. Mondal et al. [72] used the $^{12}\text{C}(^{20}\text{Ne}, ^{16}\text{O})^{16}\text{O}$ reaction, which allowed them to simultaneously obtain ANCs for all five bound states in ^{16}O, albeit with some significant discrepancies compared to other measurements. A summary of α-particle ANCs determined before and after the review of deBoer et al. [36] is given in Table 1.

In addition, the three measurements of Adhikari et al. [4], Mondal et al. [72] and Shen et al. [99] have all reported new measurements of the ground state ANC. This was highly motivated by the large discrepancy and uncertainty reported for this ANC in previous works [5,73]. While the new measurements are still inconsistent with each other, especially those of Adhikari et al. [4] and Shen et al. [99], the spread in values has decreased substantially compared to the previous measurements.

The ground state ANC has been neglected somewhat in previous studies because the direct capture for the ground state was negligible compared to previous uncertainty estimates. However, with the reduced uncertainties drawn from recent measurements, this is no longer the case as shown by Sayre et al. [96]. While effective charge term suppresses the $E1$ direct capture greatly, it would be identically zero if the charge to mass ratios of ^{4}He and ^{12}C were the same, the $E2$ component has a larger amplitude. While still relative small compared to the $E2$ subthreshold resonance contribution, their interference term is substantial. Interestingly, Shen et al. [99] showed that there are two *R*-matrix fit solutions that can equally describe the experimental data yet lead to substantially different low energy $E2$ cross sections. However, the solution using the ground state ANC of that work required an ANC for the 2^+ subthreshold state that was significantly larger than the high accuracy subCoulomb values determined by Avila et al. [11], Brune et al. [25] and Hebborn

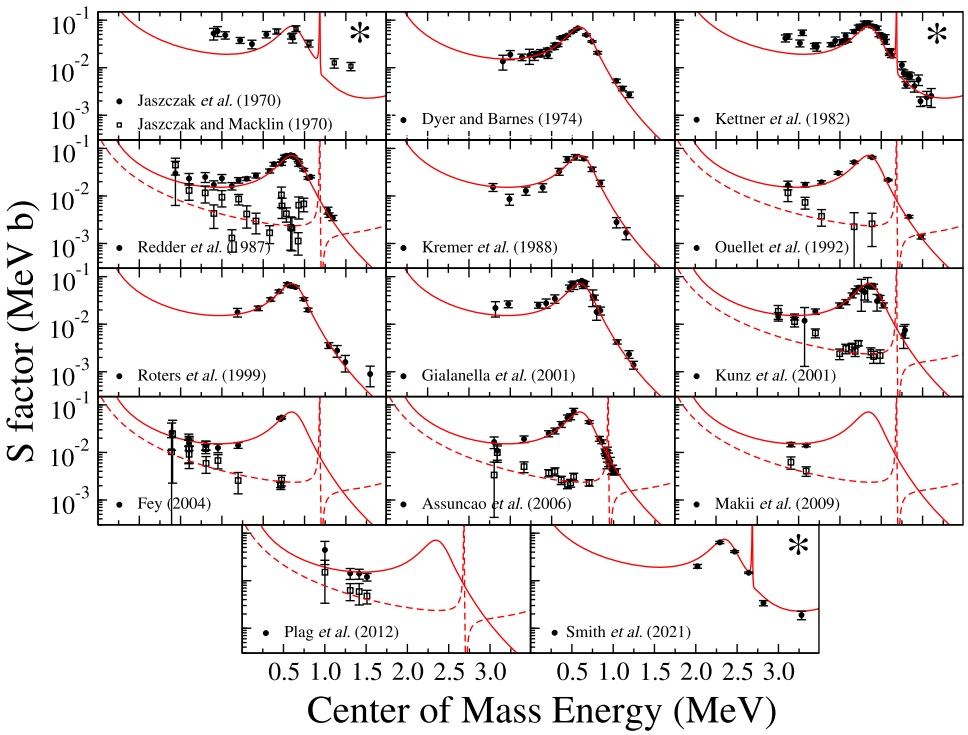

Fig. 4 Comparison of $E1$, $E2$ and total ground state cross section data for the $^{12}C(\alpha, \gamma_0)^{16}O$ reaction, where the totals are indicated by an (*). For comparison, the R-matrix fit of deBoer et al. [36] is also shown where the solid red line indicates the $E1$ contribution (except where only the total is given) and the red dashed line the $E2$ contribution. No normalization factors have been applied to the data. Figure adapted from deBoer et al. [36]

Table 1 Summary of α-particle ANCs determined by transfer measurements for bound states in ^{16}O. The table is divided into measurements made before and after the 2017 evaluation of deBoer et al. [36]

Ref.	$ANC_\alpha(fm^{-1/2})$				
	G.S.,0^+	6.05, 0^+	6.13, 3^-	6.92, 2^+	7.12, 1^-
Pre 2017					
Morais and	1200 (WS2)				
Lichtenthäler	4000 (WS1)				
[73]	750 (FP)				
Brune et al. [25]				$1.11(11)\times10^5$	$2.08(20)\times10^{14}$
Belhout et al. [14]				$1.40(50)\times10^5$	$1.87(54)\times10^{14}$
Adhikari and Basu [5]	13.9(24)				
Oulebsir et al. [84]				$1.44(28)\times10^5$	$2.00(35)\times10^{14}$
Avila et al. [11]		1560(100)	139(9)	$1.22(7)\times10^5$	$2.09(14)\times10^{14}$
Post 2017					
Adhikari et al. [4]	637(86)				
Shen et al. [99]				$1.05(14)\times10^5$	
Shen et al. [100]	337(45)				
Mondal et al. [72]	471(75)	1180(230)	152(30)	$1.03(15)\times10^5$	$5.68(85)\times10^{14}$
Nan et al. [77]					$1.59(13)\times10^{14}$
Hebborn et al. [52]		1370(58)	122(6)	$1.07(3)\times10^5$	$1.84(9)\times10^{14}$
Exp.: [11,25]				$0.98(8)\times10^5$	$1.83(16)\times10^{14}$

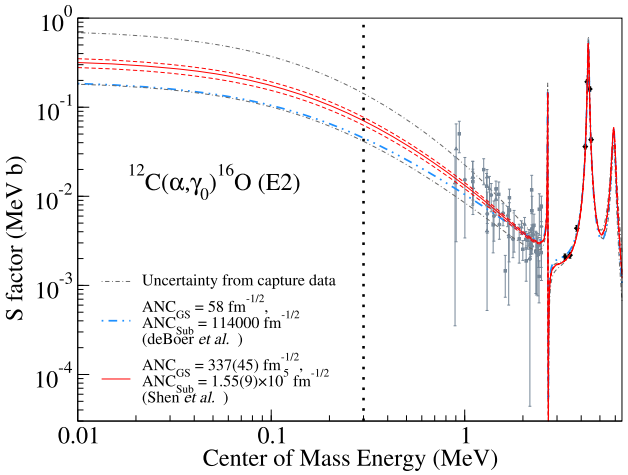

Fig. 5 Comparison of two different R-matrix fit strategies for the $E2$ component of the ground state transition in the $^{12}C(\alpha,\gamma)^{16}O$ reaction. The fit of deBoer et al. [36] uses the ANC of the 2^+ subthreshold state measured by Brune et al. [25] and then deduces a ground state ANC by fitting (blue dashed-dot-dot line), while that of Shen et al. [100] fixes the ground state ANC to the value they measured and then deduces the 2^+ subthreshold state ANC by fitting. Two solutions are found that describe the radiative capture data equally well, but each solution requires that one of the ANCs be inconsistent with an ANC from transfer measurements

et al. [52], while the solution using the 2^+ subthreshold state ANC of Avila et al. [11] and Brune et al. [25] that was found in deBoer et al. [36] requires a much smaller ground state ANC as shown in Fig. 5.

3 New nuclear theory results

Although there has been considerable recent progress with ab-initio theoretical methods, the $^{12}C(\alpha,\gamma)^{16}O$ reaction remains out of the reach of these techniques [78]. Methods that leverage the α-clustering present in ^{12}C and ^{16}O are particularly advantageous in the present case [59,64]. It appears likely that ab-initio calculations of the bound-state ANCs will become available in the near term.

Below, we discuss theoretical progress in other areas, specifically the determination of ANCs via the extrapolation of phase shifts and use of effective field theory. Both of these are essentially two-body methods. We will also point out the recent work an α clustering applied to transfer reactions Fukui et al. [48]. This analysis shows that improved theory for transfer reactions can contribute to our understanding of $^{12}C(\alpha,\gamma)^{16}O$.

3.1 ANC determinations from scattering

The idea that bound-state ANCs can be determined from the extrapolation of elastic scattering phase shifts to negative energies has a long history, going back to the 1950 paper of Bethe and Longmire [16]. The basic idea is that complicated non-analytic energy dependence of the phase shift introduced by the separation threshold and Coulomb interaction can be taken into account exactly, leaving a function that is easier to extrapolate. The works discussed below use effective range theory, or closely related functional dependences. It should also be noted that phenomenological R-matrix theory is very closely related to these methods [107].

Recent work to determine ANCs from $^{12}C + \alpha$ scattering has been published by Blokhintsev et al. [20,21], Orlov et al. [82], Ramírez Suárez and Sparenberg [88] while the work of Blokhintsev et al. [19] has investigated the reliability of the extracted ANC using an analytically-solvable model. In the most recent work [21], the extracted ANCs for the near-threshold 3^-, 2^+, and 1^- states are in good agreement with the results from transfer reactions, but the quoted uncertainties appear to be unrealistically small. It would be helpful to compare the various methods, while also including phenomenological R-matrix theory, using a consistent methodology. It should also be noted that all of these works fit the phase shift "data" of Tischhauser et al. [109], that are in fact sampled from R-matrix fits to elastic scattering differential cross sections. These results are thus not completely independent of phenomenological R-matrix theory.

3.2 Effective field theory

An Effective Field Theory (EFT) model for $^{12}C + \alpha$ scattering [7] and $^{12}C(\alpha,\gamma)^{16}O$ [8] has been developed by Ando [7,8]. For elastic scattering, this approach is equivalent to effective range theory and is thus very similar to the work described above. The results for the bound-state ANCs reported in Table IV of Ando [7] are mostly in fair agreement with the results from transfer reactions. The EFT model for the capture reaction represents a totally new phenomenological approach to describing the $^{12}C(\alpha,\gamma)^{16}O$ reaction. While the calculations described in Ando [8] do not describe the experimental data as well as phenomenological R-matrix fits do, the EFT approach lends itself to systematic improvement, for instance, the EFT expansions can be extended to higher order and broader energy ranges can be considered. One can expect further progress with this approach in the future.

3.3 ANC of ^{6}Li

As discussed in Sect. 2.3, α-particle transfer reactions, such as $(^6Li, d)$ and $(^7Li, t)$, have been extensively used to constrain ANCs relevant for astrophysics. These evaluations of ANCs carry uncertainties that result from experimental and theoretical uncertainties associated with the reaction model used to analyze the data. Typically, α-particle transfer reactions are seen as a three-body problem composed of an inert

cluster, which interacts through pairwise interactions. The reaction dynamics is then usually described with the Distorted Wave Born Approximation (DWBA), which assumes that the reaction occurs in one step [95,108]. The ANC of the state of interest is then obtained by normalizing the theoretical predictions to the transfer data. The DWBA reaction model and its inputs all carry uncertainties that are in general difficult to quantify, e.g., because of the scarcity of nucleus-nucleus optical potentials and reliable measurements of precise bound-state radii that could be used to constrain binding potentials.

In a recent work, Hebborn et al. [51] have performed a first-principle prediction of the ^{6}Li properties. They used validated nucleon-nucleon and three-nucleon interactions derived within the framework of chiral effective field theory and the ab initio no-core shell model with continuum. This theoretical method has the advantage of treating the α-d scattering dynamics and bound ^{6}Li product on an equal footing. Their predictions agree within uncertainties with available data: $\alpha(d,\gamma)^{6}$Li S-factor, α-d scattering observables and ^{6}Li ground state magnetic moment. However, they found a s-wave α-d ANC for the ^{6}Li ground state that is 15% larger than previous evaluations [18]. Compared to experimental determination of ANCs, these uncertainties are more straightforwardly quantifiable, as they only take as input nucleon-nucleon interactions. It is therefore crucial to push such first-principles predictions to heavier systems, such as ^{16}O [59].

Although predicting the structure and reaction properties of ^{16}O starting from nucleonic degrees of freedom is still out of reach, one can leverage ab initio predictions of light systems to improve the analysis of reaction data. In particular, the aforementioned ^{6}Li prediction was used to extract ANCs of ^{17}O and ^{16}O from (^{6}Li, d) transfer data [52]. Their reanalysis lead to smaller ANCs with reduced errors for ^{17}O and ^{16}O states. These new evaluations of ^{17}O and ^{16}O ANCs further resolve the discrepancies between two recent evaluations of ^{13}C(α, n)^{16}O reaction rates and lead to a 21% reduction in the ^{12}C(α, γ)^{16}O S-factor at low energy with respect to deBoer et al. [36]. To further improve the ANC determination, it would be desirable to leverage first-principle predictions of other light systems, e.g. ^{7}Li, to analyze various transfer data, e.g., (^{7}Li, t). Moreover, it would be valuable to improve few-body models used to analyze transfer data, e.g., by going beyond the one-step DWBA description.

3.4 Phenomenological R-matrix

While phenomenological R-matrix analysis has been a standard method for many years [37,63], its mathematical complexity and formal parametrization have often made it hard to access. In recent years, several attempts have been made to make this method more practically viable, most notably the increased availability of sophisticated R-matrix codes [12,119] and methods for reparameterizing the fit parameters into something more akin to classical level parameters [24,39,85]. In particular, the `AZURE2` code used by deBoer et al. [36] makes use of the alternative parameterization of Brune [24].

One of the other really challenging aspects of R-matrix analysis is the extraction of reliable uncertainties from the fitting. This is not a problem unique to R-matrix analysis, but a general challenge when fitting any type of model to experimental data. However, the issues are often magnified for R-matrix fits because they often include many fit parameters and large amounts of experimental data. Further, the mathematical operations that need to be performed can lead to long calculation times. These issues have been somewhat alleviated by ever increasing computational power but it is still a major roadblock in performing these types of calculations. These computational times are further slowed by the need to convolute the R-matrix cross sections with experimental resolution functions. Thus improvements in these areas of R-matrix calculations are highly desirable.

One of the main objectives of deBoer et al. [36] was to provide the community with a reaction rate based on more statistically rigorous methods. This was accomplished by randomly sampling the experimental data sets based on their quoted uncertainties and refitting many thousands of times. While this method produced much improved results, in the interim, more sophisticated Bayesian type algorithms have begun to be implemented for R-matrix analysis uncertainty quantification [74,80,81]. These types of algorithms are important on a very practical level, because they make it easier to implement different sources of uncertainty into the uncertainty analysis. A good example are the differential cross section data of Plag et al. [86]. They were not included directly in the R-matrix analysis of deBoer et al. [36], because the uncertainties on the angles of measurement (see Fig. 13) were not easily implementable in that analysis. While these types of analyses have still not yet been implemented for such a data intensive analysis as the ^{12}C(α, γ)^{16}O R-matrix analysis of deBoer et al. [36], ever increasing computational capabilities mean that it will soon be within reach.

4 Observational constraints

4.1 Theoretical considerations

Fred Hoyle [55] was the first to understand in 1954 the importance of the competition between the two key processes that control He burning: "It can be shown that reaction ^{12}C(α,γ)^{16}O is the most effective in destroying ^{12}C. Hence, to decide how far ^{12}C accumulates, it is necessary to compare the rates of the two nuclear reactions 3α and ^{12}C(α,γ)^{16}O".

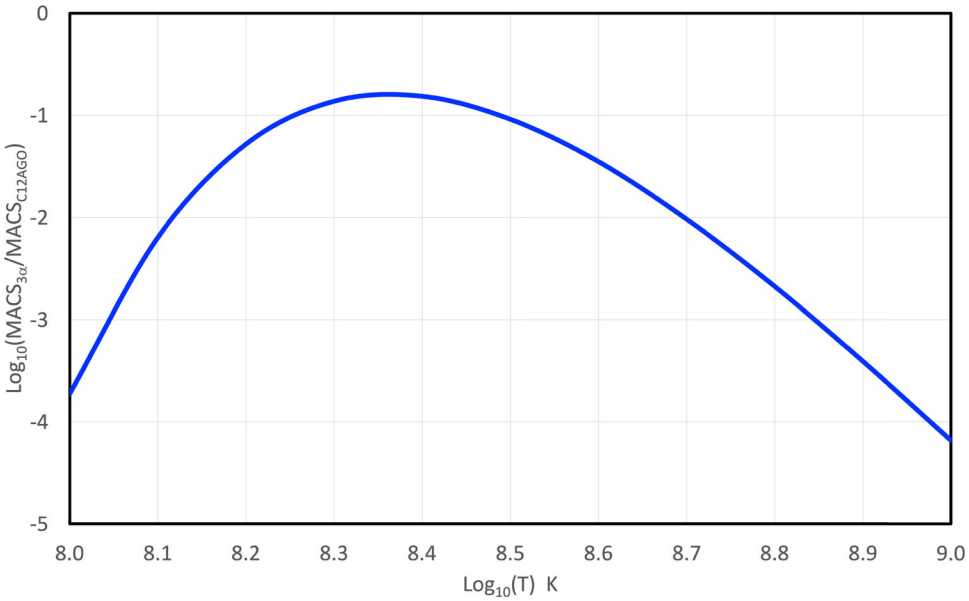

Fig. 6 Logarithmic ratio of the 3α MACS to the $^{12}C(\alpha,\gamma)^{16}O$ one

Approximately 20 years later Arnett [9], in the 1973 issue of the Annual Reviews of Astronomy and Astrophysics, writes: "The rate of the $^{12}C(\alpha,\gamma)^{16}O$ during hydrostatic helium burning is of vital interest for explosive nucleosynthesis. It is this process that determines the abundances of ^{12}C and ^{16}O in the star and thereby sets the stage for explosive burning... The rate is determined by the 7.115 MeV level in the ^{16}O compound nucleus. At present the reduced width θ_α^2 of this resonance for α captures is *not known*."

Let us start the discussion by reviewing a few well known facts: the energetics in He burning is totally dominated by the two processes 3α and the $^{12}C(\alpha,\gamma)^{16}O$ reaction. Both release a similar amount of energy per single fusion, the first one 7.275 and the second 7.162 MeV. While the rate of the 3α process scales as $Y_a^3\ \rho^2/6$, the $^{12}C(\alpha,\gamma)^{16}O$ reaction scales simply as $Y_{^{12}C}\ \rho$. Figure 6 shows the ratio between the 3α process Maxwellian-Averaged Cross Section (MACS) and that of the $^{12}C(\alpha,\gamma)^{16}O$ reaction between 0.1 and 1 GK. The figure shows very clearly that the $^{12}C(\alpha,\gamma)^{16}O$ cross section dominates over the 3α process and hence the reaction rate of the 3α process may overcome that of the $^{12}C(\alpha,\gamma)^{16}O$ reaction only when the $Y_a^3\ \rho/6 > Y_{^{12}C}$. For each given He core mass (MHE), not total mass, this condition is certainly verified at the beginning of He burning when the He abundance is high and the C abundance is very low. As He burning proceeds, the density rises somewhat but the strong dependence of the rate of the 3α process on the He abundance, associated to the progressive increase in the ^{12}C abundance, leads inevitably to a progressive increase in the role of the $^{12}C(\alpha,\gamma)^{16}O$ reaction until the two rates settle at equilibrium. Once ^{12}C reaches its equilibrium abundance, given by $Y_{^{12}C} = Y_a^3\ \rho/6\ (MACS_{3\alpha}/MACS_{^{12}C(\alpha,\gamma)^{16}O})$, it will maintain it up to central He exhaustion. For this reason the C abundance rises during the first part of central He burning and then drops progressively up to the exhaustion of He. Vice versa, the dependence of the amount of C left by the He burning on the He core mass is determined by the fact that the typical temperature of the He burning scales directly with MHE while the typical density scales inversely with MHE. The consequence is that the more massive the MHE, the higher the He abundance at which ^{12}C settles on its equilibrium abundance and hence the level of ^{12}C in the He exhausted core (the CO core) scales inversely with the $^{12}C(\alpha,\gamma)^{16}O$ cross section. It also should be remembered that the amount of energy provided by central burning does *not* depend on the efficiency of the key nuclear reactions but is fixed by the current mass (initial, He or CO depending on the evolutionary phase) and that the amount of energy provided by the two cross sections are similar, the fact that the $^{12}C(\alpha,\gamma)^{16}O$ reaction consumes just one α-particle instead of three implies that the lifetime of He burning scales directly with the $^{12}C(\alpha,\gamma)^{16}O$ cross section.

The fact that the $^{12}C(\alpha,\gamma)^{16}O$ cross section directly influences He burning (lifetime and path in the HR diagram) implies that there is a possibility, at least in principle, that the efficiency of this reaction can be determined by looking at stars currently burning He in their cores, like the Cepheids: Iben [56] first, and Brunish and Becker [26] later, discussed the role of an enhanced $^{12}C(\alpha,\gamma)^{16}O$ cross section on the properties of intermediate mass stars finding that the higher the cross section of this process the more extended the blue loop experienced by stars in the HR diagram, which influences the expected number of stars in the Cepheid state, as well as their masses. However, a few years later, Umeda et al. [114] and Bono et al. [22] obtained the opposite result, i.e. that an increase of the $^{12}C(\alpha,\gamma)^{16}O$ cross section does not affect the evolutionary properties of intermediate mass

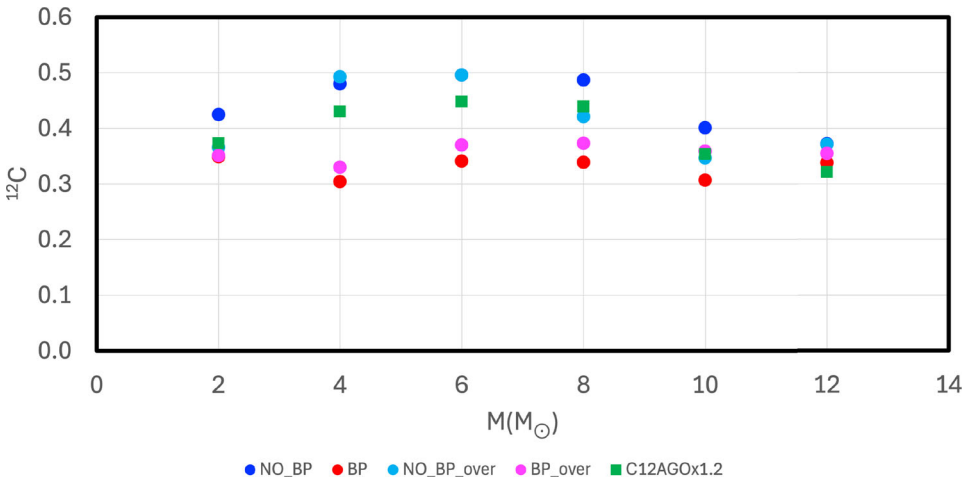

Fig. 7 Mass fraction of the ^{12}C abundance left by He burning as a function of the initial mass for five sets of models. The blue dots represent our standard case, i.e. all models are computed without any kind of overshooting in H burning, the Kunz et al. [62] $^{12}C(\alpha,\gamma)^{16}O$ cross section and the induced overshooting in He burning. The green dots represent models computed as the reference ones but the $^{12}C(\alpha,\gamma)^{16}O$ cross section is now the upper limit proposed by Kunz et al. [62]. The red dots represent models computed as the reference ones but without inhibiting the BPs. The cyan dots represent models computed as the reference ones but adopting 0.5 Hp of overshooting in central H burning. The magenta dots are models computed by summing up both the overshooting in central H burning and the BPs in He burning

stars and consequently of the blue loops. It must be noted, however, that the occurrence, elongation and duration of blue loops is still not properly understood, as demonstrated by the wide range of differing results presented by Renzini [90], Stancliffe et al. [103] and references therein.

The role of ^{12}C abundance left over by He burning on the evolution of stars beyond He burning depends on the mass. We can identify three broad ranges: the low and intermediate mass plus a fraction of the Super Asymptotic Giant Branch stars (i.e. stars that leave a CO or a CONe remnant), massive stars that explode as core collapse supernovae and the very massive stars close to the Pulsation Pair Instability (PPI) limit or Pair Instability limit (PI). In all these cases the influence of the $^{12}C(\alpha,\gamma)^{16}O$ reaction on the evolutionary properties of stars is indirect, in the sense that their evolution is controlled by the amount of ^{12}C left behind by He burning that, in turn, is determined by the interplay of several phenomena, none of them being well known, including the $^{12}C(\alpha,\gamma)^{16}O$ reaction.

In order to directly connect the amount of C left by He burning to the $^{12}C(\alpha,\gamma)^{16}O$ cross section it would be necessary to establish a one to one relation between the $^{12}C(\alpha,\gamma)^{16}O$ cross section and the C left by He burning. Unfortunately such a relation does not exist. As an example, Fig. 7 shows the amount of C left over by He burning for stars between 2 and 12 M$_\odot$ and four different treatments of the convection (blue, red, cyan and magenta dots) plus a set of models computed by adopting the upper limit of the $^{12}C(\alpha,\gamma)^{16}O$ cross section provided by Kunz et al. [62].

Before discussing Fig. 7, it is important to emphasize that the extension of the convective core during He burning is particularly complex, owing to the strong dependence of the opacity on its chemical composition. The adoption of simply the Schwarzchild criterion leads to an nonphysical discontinuity in the radiative gradient at the border of the convective core that is avoided by including what Castellani et al. [28] called *induced* overshooting. Towards the end of He burning, when the central He abundance drops below approximately 0.1, the ingestion of even a modest amount of additional He in the core leads to what Caputo et al. [27] called Breathing Pulses (BP), i.e. the sudden growth of the convective core that again raises the central He abundance by up to a factor of 0.2−0.4 by mass fraction (sometimes even more). See, for example, the papers by Castellani et al. [28], Caputo et al. [27] and Imbriani et al. [57], who discuss in great detail all the phenomena briefly sketched above.

The real extension of the convective core in general, but also more specifically the existence or not of the instabilities (the BPs) that occur towards the end of He burning, are highly questionable because, as is well known, the treatment of convection in classical 1D models is far from robust and must be guided by the comparison between models and observational data to fix the proper size of the convective regions. For this reason, Caputo et al. [27] proposed a method called the "Red Giant Branch Clock" to determine the extension of the mixing in central He burning by analyzing the distribution of stars in well observed Galactic Globular Clusters. A similar approach was followed by Constantino et al. [34] and Constantino et al. [35], who concluded that the BP do not occur in nature. However, we notice that in these two papers the scheme they adopt for the mixing actually allows several BPs

to occur even if they are partly inhibited by means of a free parameter. Hence we think that, at least at present, it is still unclear which is the real extension and temporal evolution of the convective core in central He burning.

Coming back to the models shown in Fig. 7, the blue dots represent our standard case, i.e. all models are computed without any kind of overshooting in H burning, the Kunz et al. [62] $^{12}C(\alpha,\gamma)^{16}O$ cross section and the induced overshooting in He burning. The green dots represent models computed as the reference ones but with the upper limit of Kunz et al. [62]'s $^{12}C(\alpha,\gamma)^{16}O$ cross section. The red dots represent models computed as the reference ones but without inhibiting the BPs: it is quite evident that the extramixing triggered by the BPs towards the end of the He burning reduces the final C abundance more than the upper limit provided by Kunz et al. [62]. The cyan dots represent models computed as the reference ones but 0.5 Hp of overshooting has been taken into account in central H burning: in this case the situation is non monotonic in the sense that in a few cases the overshooting alters the final outcome of C at central He exhaustion more than a variation of the $^{12}C(\alpha,\gamma)^{16}O$ rate up to its upper limit, while in other cases the final C abundance is not affected by the overshooting. The magenta dots are models computed by summing up both the overshooting in central H burning and the BPs in He burning. The result is that these models do not differ significantly from those obtained by including the BPs but not the overshooting in H.

Fortunately stars more massive than 12 $M_\odot$ or so do not suffer from the possible presence of BPs because their dependence on the opacity of the chemical composition reduces as the He burning temperature increases. There is however another phenomenon that may significantly affect the final chemical composition of the core He burning, and this is rotation. Figure 19 in Limongi and Chieffi [65] shows the dramatic impact rotation has on the final C abundance at the end of He burning in massive stars. Note that we do not have rotating models of low and intermediate mass stars but it is very probable that in that mass range rotation may significantly affect the final amount of C.

Imbriani et al. [57] discusses, in great detail, the role played by the $^{12}C(\alpha,\gamma)^{16}O$ reaction in contributing to the final abundance of ^{12}C at central He exhaustion over a mass range that covers all masses between 0.8 $M_\odot$ and 25 $M_\odot$ also addressing the role of the $^{12}C(\alpha,\gamma)^{16}O$ reaction on the final explosive yields obtained for 25 $M_\odot$ stellar models.

Further, both the thermal and mechanical instabilities may only reduce the amount of C left by He burning, simulating therefore a $^{12}C(\alpha,\gamma)^{16}O$ rate more efficient than that assumed by the *recommended* one. This means that, if the comparison between models and observational data would lead to a determination of the C abundance *higher* than the one obtained by adopting the reference rate, with no overshooting and no rotation induced instabilities, this would really imply a quite strong correlation between the $^{12}C(\alpha,\gamma)^{16}O$ cross section and final abundance of C. Note however that mass loss should not be so strong that it would reduce the mass size of the He core in He burning because such an occurrence would push in the opposite direction, i.e. towards a higher final C abundance.

Keeping in mind the general warning about the (lack of) robustness between the $^{12}C(\alpha,\gamma)^{16}O$ cross section and the amount of C left by He burning, we discuss briefly the role of C in stars that do not experience any further burning beyond He but leave a remnant. According to the chemical composition of the degenerate core, White Dwarfs (WD) may be grouped basically in three main categories: the WD_{CO}, i.e. the ones mainly formed of C and O, the WD_{CONe}, i.e. those made mainly of C, O and Ne, and the WD_{ONe} that are those mainly composed of O and Ne. The lifetime of a WD in the cooling sequence is sensative to the amount of C present in the electron degenerate core. Salaris et al. [94], by computing the cooling sequence of a 0.61 $M_\odot$ WD, found that its lifetime scales inversely with the rate of the $^{12}C(\alpha,\gamma)^{16}O$ reaction, i.e. directly with the amount of ^{12}C present in the CO core. Straniero et al. [104] studied the variable WD GD 358 finding that it must have a quite low C/O ratio but they could not provide any constraint on the $^{12}C(\alpha,\gamma)^{16}O$ cross section because of the competing influence of mixing (and of the BPs, Castellani et al. [28] and Imbriani et al. [57]) in controlling the final abundance of ^{12}C. Fields et al. [45] studied the evolution of a 3 $M_\odot$ star by varying the cross section using a Monte Carlo technique within their range of uncertainty finding that the $^{12}C(\alpha,\gamma)^{16}O$ cross section is one of the processes that most contributes to the properties of this star at the beginning of the Thermally Pulsing phase.

Another possibility for determining the amount of C present in the core of WDs comes from astroseismology (see, e.g., Metcalfe et al. [70], Fontaine and Brassard [46], Metcalfe [71], Bischoff-Kim [17]). In fact, the analyses of the frequencies of oscillations observed in a number of WDs allows for the determination of the amount of C present in the CO core as well as the location of the C bump that forms just outside the border of the convective core at the beginning of the Early Asymptotic Giant Branch phase (see the next section). It must also be remembered that a fraction of these WD are probably the nursery of Type Ia Supernovae and thus also in this case the amount of ^{12}C left by He burning plays a role in determining the properties of the shock wave in its passage towards the surface.

In the range of the massive stars, the amount of ^{12}C left by He burning is crucial in controlling all the advanced burning phases of a massive star because it is *the* fuel that feeds the C burning (core and shell burning) and therefore determines the number, extension and duration of the C convective zones that develop prior to the final collapse. Chieffi and Limongi [32] have shown, on a very fine mass grid extending between 12 and 28 $M_\odot$ how the complex sequence of convective C shell

Table 2 Comparison of simulations of a rotating pure He star using the $^{12}C(\alpha, \gamma)^{16}O$ reaction rate of Kunz et al. [62] and the mass loss formalism of Nugis and Lamers [79]

$^{12}C(\alpha, \gamma)^{16}O$ rate	Mass loss	Overshooting	0	200 km/s	400 km/s
[62]×0.8	[79]	0.5 Hp	0.206	0.202	0.192
[62]	[79]	0.5 Hp	0.148	0.144	0.136
[62]×1.2	[79]	0.5 Hp	0.103	0.100	0.093
[62]	[79]	–	0.149	–	–
[62]	–	–	0.093	–	–
[62]	–	0.5 Hp	0.097	–	–

burning influences the final compactness of a star and hence its capability to explode or implode. An analogous analysis was performed by Sukhbold et al. [105] even if their results showed a wide random scatter on very small mass intervals. The final structure of a star at the onset of the core collapse, sculpted by the C core and shell burning, fixes the position and extension of the last C convective shell, therefore also controlling the yields of the elements mainly produced by C burning (i.e. Ne, Na, Mg, Al). It should also be remembered that Ne burning is largely affected by the ^{12}C left by He burning because C burning leaves an amount of Ne which is comparable to that of C (in mass fraction). Hence the lower the amount of C available for the advanced burning, the lower the amount of Ne, so that the nuclei produced by explosive Ne burning are clearly affected by the amount of C available. Since the $^{12}C(\alpha,\gamma)^{16}O$ cross section influences the amount of C left by He burning, several authors have tried to fix the correct rate of this process by requiring that the yields of the intermediate mass nuclei provided by a generation of massive stars of solar metallicity preserve, as close as possible, the relative solar proportions, see e.g. Tur et al. [111], Tur et al. [112], Weaver and Woosley [116] and West et al. [118]. It is also worth noting that the yields of the γ-ray emitters ^{26}Al, ^{60}Fe and ^{44}Ti are affected by the amount of C left by He burning, see Tur et al. [113].

In recent years the idea has been proposed Brown et al. [23], Farmer et al. [41,42], Mehta et al. [69], Takahashi [106] and Renzo and Smith [91] that the $^{12}C(\alpha,\gamma)^{16}O$ cross section could be reasonably well fixed by requiring that the theoretical lower limit of the stars that enter the PI region fits the lower limit of the expected gap in the BH mass distribution observed by the GW antennas of the Ligo/Virgo collaboration. By way of this gap, the softening of the EOS caused by the high equilibrium abundance of e^+e^- pairs that force the adiabatic index Γ_1 to drop below 4/3 in a consistent fraction of the core is determined, an occurrence that leads to an early explosion that does not leave any remnant. Also, in this case the reliability of this approach depends on the solidity of the relation between the $^{12}C(\alpha,\gamma)^{16}O$ cross section and the amount of C left over by He burning.

Obviously, we cannot present here an extended set of models but we want to show, as an example, how the C left by the He burning in a pure He star of $60M_\odot$ (solar composition) changes by including some angular momentum and/or some overshooting. It should be carefully noted that the effects of rotation on a pure He star are completely different from those that would occur in the presence of a H rich envelope. The reason for this is the lack of entanglement between the convective core and the base of the H burning shell established by the rotation induced instabilities whose main effect is to convert part of the freshly produced ^{12}C into ^{14}N, see e.g. Chieffi and Limongi [31], Limongi and Chieffi [65] and Roberti et al. [92].

Table 2 summarizes some key information from these tests. The basic model is the one shown in the second row of the table: it has been computed assuming the Schwarzchild criterion fixes the border of the convective core plus an overshooting of 0.5 Hp, the adopted mass loss rate is the one provided by Nugis and Lamers [79], and the $^{12}C(\alpha,\gamma)^{16}O$ cross section is again the one provided by Kunz et al. [62]. Rotation is included as described by Chieffi and Limongi [31] and Limongi and Chieffi [65]. The second row in Table 2 shows that in the non-rotating case, the mass fraction of C left by He burning amounts to $X_C = 0.148$. According to Kunz et al. [62], an upper and lower limit that bracket the possible range of values for this cross section may be obtained by multiplying the reference rate by 1.2 and 0.8, respectively. The results for the non rotating models are shown in the first and third row of Table 2. These models show a variation of a factor of two in the C abundance between the lower and upper limits. The inclusion of a moderate amount of rotation shows that the influence of rotation (at least for this specific case) does not significantly modify the amount of C left by He burning. Also the overshooting does not play a relevant role (comparison between the second and the fourth row) and this is easily understandable because an overshooting of 0.5 Hp adds $\approx$1 $M_\odot$ to a convective core of 50 $M_\odot$, i.e. a very modest increase in the size of the convective core provided by the Schwarzchild criterion. Also, the modest effect of rotation can be understood by considering that the region above the convective core amounts to less than 10 $M_\odot$ and hence the mechanical instabilities meridional circulation and shear do not have much room to operate. The same result is visible by comparing the fifth and sixth rows (both computed

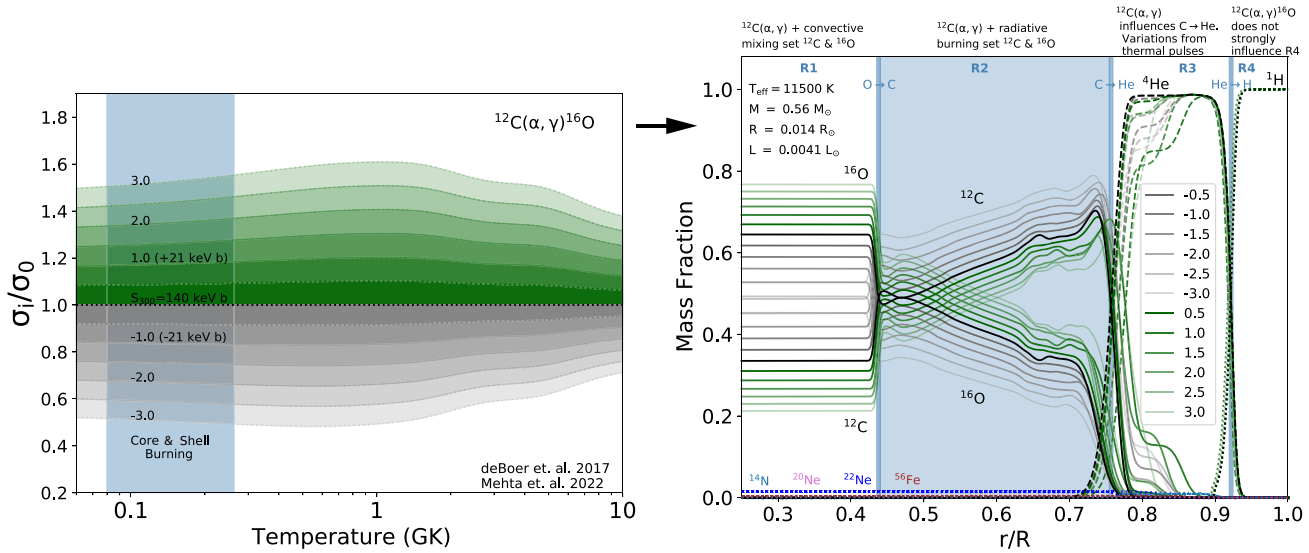

Fig. 8 *Left:* The ^{12}C(α, γ)^{16}O reaction rate ratios, σ_i/σ_0, as a function of temperature. Here, σ_i spans −3.0 to +3.0 in 0.5 step increments, with σ_0 being the nominal rate of deBoer et al. [36]. Negative σ_i are gray curves and positive σ_i are green curves with the $\pm 1, 2, 3$ σ_i curves labeled. The blue band shows the range of temperatures encountered during core and shell He burning. *Right:* Mass fraction profiles of the evolutionary white dwarf models resulting from the ^{12}C(α, γ)^{16}O reaction rate uncertainties σ_i after each model has cooled to a photosphere temperature of 11,500 K. The nominal $\sigma = 0$ reaction rate is represented by the black curve, negative σ_i are gray curves and positive σ_i are green curves. Solid curves are for ^{12}C and ^{16}O, dashed curves are for ^{1}H and ^{4}He. The trace isotopes ^{14}N, ^{20,22}Ne, and ^{56}Fe are also labeled as are key regions and transitions. Figure adapted from Chidester et al. [29]

without mass loss) computed respectively with and without overshooting. Actually the major influence on the amount of C left by He burning comes from mass loss. A comparison between the second and the sixth rows shows that mass loss (in this case the NL one) may significantly affect the final value of C after central He exhaustion. The reason is that the central temperature and density depend on the current value of the He core mass and hence they readjust continuously as the He core mass changes. Of course it also matters when the mass loss occurs: if it was caused by a binary interaction it may occur at any stage during He burning. Its effect will therefore depend on the specific mass loss rate and on the specific moment of the central He burning phase in which it activates. Therefore, even if the central He burning of the very massive stars is not affected much by (a moderate amount of) rotation or overshooting, mass loss (that is still one of the major uncertainties in the modeling of the stars in general) or mass transfer in a binary system, may alter the final outcome of C.

The discussion above has shown that it is presently possible to derive valuable information about the amount of C left by He burning in a quite large number of cases spread over a very wide mass range. However, the successive step of linking the amount of C to the cross section of the ^{12}C(α,γ)^{16}O reaction must be performed with great caution. In general it would be useful to provide the amount of C left by He burning that comes out of the comparison between models and observational data first and then provide an estimate of the ^{12}C(α,γ)^{16}O cross section associated with that C abundance.

4.2 Variable white dwarfs

Variable carbon-oxygen white dwarfs offer a potential signature of the current experimental ^{12}C(α, γ)^{16}O reaction rate probability distribution function through their observed pulsation periods [29,30]. Adiabatic gravity-modes trapped by the interior carbon-rich layer offer potentially useful signatures because they form during the evolution of low-mass stars under radiative helium burning conditions, mitigating the impact of convective mixing processes. Figure 8 indicates the average spread in relative period shifts of $\Delta P/P \simeq \pm 2\%$ for the identified trapped g-modes over the $\pm 3\sigma$ uncertainty in the ^{12}C(α, γ)^{16}O reaction rate probability distribution function [29,30] across the effective temperature range of observed variable white dwarfs and for different white dwarf masses, He shell masses, and H shell masses. The g-mode pulsation periods of observed white dwarfs are typically given to 6–7 significant figures of precision. This suggests that an astrophysical constraint on the ^{12}C(α, γ)^{16}O reaction rate could, in principle, be extractable from the period spectrum of observed variable white dwarfs.

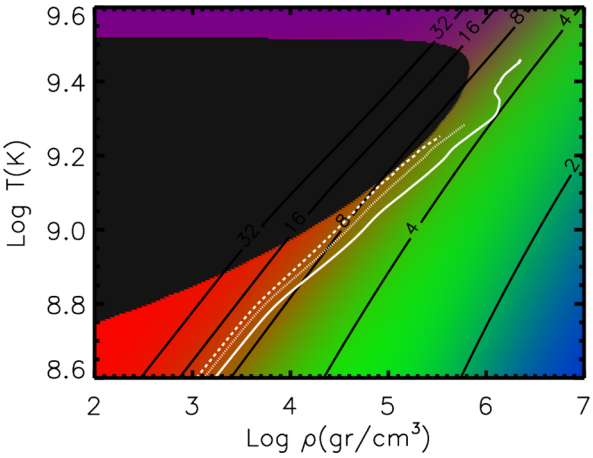

Fig. 9 The blue, green, red and violet colors in the background mark the regions where the electron degeneracy, the ideal gas, the radiation and a combination of radiation and e^+e^- pairs, respectively, dominate while the black area marks the unstable region where all three adiabatic exponents, Γ, drop below 4/3. The solid, dotted and dashed white lines show part of the evolutionary path of the center of a 40, 60 and 80 $M_\odot$star, respectively

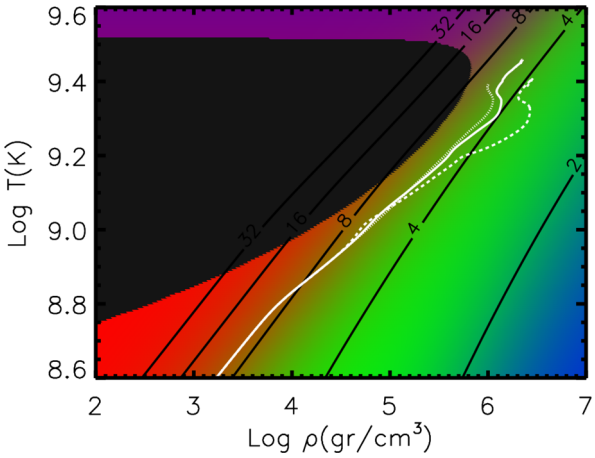

Fig. 10 As Fig. 9, but the solid, dotted and dashed white lines indicate part of the evolutionary path of the center of a 40 $M_\odot$star: the solid line refers to the reference 40 $M_\odot$ star, while the dotted and dashed lines refer to models computed by doubling and halving the $^{12}C(\alpha,\gamma)^{16}O$ reaction rate, respectively

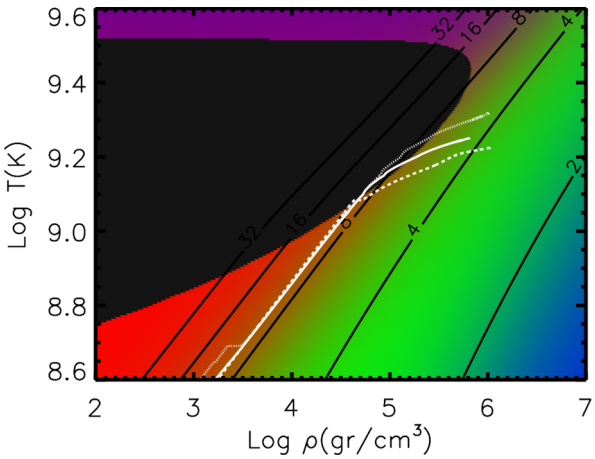

Fig. 11 As Fig. 9, but the solid, dotted and dashed white lines show part of the inner structure of a 40 $M_\odot$ star at the onset of O burning: the solid line refers to the reference 40 $M_\odot$ star while the dotted and dashed lines refer to models computed by doubling and halving the $^{12}C(\alpha,\gamma)^{16}O$ reaction rate, respectively

4.3 Massive stars

The $^{12}C(\alpha,\gamma)^{16}O$ reaction also plays a crucial role in the understanding of the black hole mass gap expected in the range of masses that enter the (pulsational) pair instability region. Several papers have been devoted to a careful analysis of the physical phenomena that are triggered when a fraction of a star enters the unstable region where the formation of a large number of e^+e^- pairs absorb the energy gained by the gravitational contraction preventing the growth of a pressure gradient able to counterbalance the contraction. We refer the reader to the papers by Refs. [13,41,42,101,120], who addressed, in great detail, the physical conditions under which a star becomes unstable and the role played by the $^{12}C(\alpha,\gamma)^{16}O$ reaction in this respect. Here we provide a brief review of the role of this nuclear cross section in determining the minimum mass that enters the pulsational pair instability region.

Let us look at Figs. 9, 10 and 11: all of them show in the background the regions of the Log(T)–Log(ρ) plane where the electron degeneracy (blue area), the ideal gas (green area), radiation (red area) and a combination of radiation and e^+e^- pairs (violet) dominate. The black area marks the unstable region where all three adiabatic exponents, Γ, drop below 4/3. If a large fraction of the interior of a star enters the unstable region marked in black, the core begins to oscillate and such oscillations may either lead to the ejection of part of the mantle or to an explosion that does not leave any remnant. The three figures also show a few lines that indicate the value of the entropy in units of Boltzmann constant and per nucleon.

Let us start with a review of a few well know basic properties of the evolution of massive stars. The more massive a star, the lower the density at each fixed temperature and hence the higher the entropy. Figure 9 shows the well known path of a massive star in the Log(T_c)–Log(ρ_c) plane: the white solid, dotted and dashed lines refer, respectively, to three pure He cores of 40, 60 and 80 $M_\odot$. Note that each model bends towards lower entropy values as it climbs towards higher temperatures and that such a bending is more pronounces in less massive stars. The reason for this is that the amount of C left by the He burning scales inversely with the He core and the smaller the amount of C at central He exhaustion, the faster the the C burning shell advances, the faster the contrac-

tion of the core and hence the smaller the amount of entropy lost by the neutrinos.

Figure 10 shows, vice versa, the evolution of three 40 $M_\odot$ stars in the Log(T_c)–Log(ρ_c) plane: the solid line refers to the model computed by adopting the Kunz et al. [61] rate, while the dotted and dashed ones were computed by multiplying and dividing the rate by a factor of two, respectively. Figure 10 clearly shows that the lower the rate the lower the central entropy. The reason for this is that, the lower the rate, the larger the amount of C left by He burning, the slower the advancing of the C burning shell and hence the larger the entropy carried away by the neutrinos. So it is clear why the larger the $^{12}C(\alpha,\gamma)^{16}O$ reaction rate, the closer the core of a massive star is to the instability region.

However, the path of a star in the Log(T_c)–Log(ρ_c) plane is not the most clever way to understand if a portion of a star significantly enters the unstable region. To really appreciate this, it is necessary to look at Fig. 11. This figure shows *not* the temporal evolution of the central temperature and density but, instead, the structural relation between temperature and density within the core of the 40 $M_\odot$ star at the beginning of O burning. The solid line indicates the reference case while the dotted and dashed lines those where the higher and lower $^{12}C(\alpha,\gamma)^{16}O$ reaction rates are used. It is evident that the model computed with the highest rate is the one that penetrates more effectively into the unstable region while the one computed with the lowest. This result therefore shows very clearly why and how this nuclear cross section may affect the minimum mass that enters in the Pulsational Pair Instability regime.

Even if this is true in principle, however, we want to note that an increase of the $^{12}C(\alpha,\gamma)^{16}O$ reaction rate has a much smaller effect than a reduction of this nuclear cross section: the reason is that the amount of C left by He burning in the reference case is already very low (less than 0.1 by mass fraction) and hence an additional reduction does not change the evolution of the core tremendously. Vice versa, a lower nuclear cross section has room to significantly increase the amount of C left by He burning, and thus has a larger impact on the evolution of a star. As a last comment on this topic we remind the reader that the $^{12}C(\alpha,\gamma)^{16}O$ cross section is not the only critical quantity responsible of the final amount of ^{12}C at central He exhaustion; other equally important actors include the instabilities, both thermal and mechanical (i.e. standard convection and rotation).

As discussed in Sects. 2 and 3, there are still significant uncertainties associated with the $^{12}C(\alpha,\gamma)^{16}O$ reaction rate that directly effect impact the uncertainty on the size of the black hole mass gap. For instance, Shen et al. [100,101] measured the asymptotic normalization coefficient (ANC) for the ^{16}O ground state (GS) using the $^{12}C(^{11}B,^{7}Li)^{16}O$ transfer reaction. This ANC is believed to significantly impact the $^{12}C(\alpha,\gamma)^{16}O$ reaction rate by constraining the external capture to the ^{16}O ground state, which in turn affects the high-energy tail of the 2^+ subthreshold state. The results indicate an increase of up to 21% in the total reaction rate compared to the recommendation of deBoer et al. [36] (see Fig. 5). This change leads to a decrease of approximately 12% at the lower edge and 5% at the upper edge of the predicted boundaries for the black hole mass gap as shown in Fig. 12.

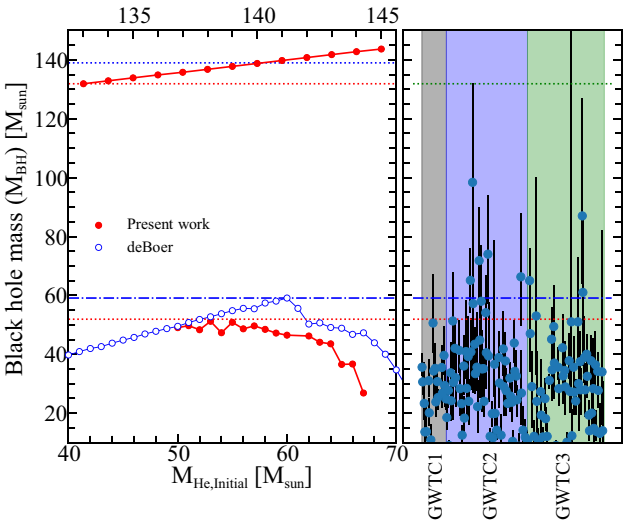

Fig. 12 Black hole mass as a function of the initial helium core mass with respect to the $^{12}C(\alpha,\gamma)^{16}O$ reaction rate. The blue circles with the line represent the values obtained using the rates from deBoer et al. [36], Mehta et al. [69], while the red dots with the line represent those obtained using the rates given by Shen et al. [100,101]. The boundaries of the black hole mass gap are presented by the blue dash-dotted lines and red dotted lines respectively. The right panel shows the masses of the black hole from the first, second and third Gravitational-Wave Transient Catalog (GWTC1, GWTC2 and GWTC3) with the restriction that the median estimated mass of the primary is $\geq 10\,M_\odot$. The uncertainty bars represent 90% confidence intervals [1–3]

5 Future prospects and experimental directions

In recent years, new direct measurements to lower energy have reached something of a road block, unable to push below 1 MeV center of mass energy. For this reason, few new measurements have been made in recent years, yet several new paths of investigation are being considered. Most straightforward, yet still extremely difficult, are new measurements with high-intensity accelerators at underground laboratories. While beam induced background remains one of the primary hindrances, these low background environment laboratories still may provide a better environment for measurements, coupled with the infrastructure and targetry techniques for high beam intensity measurements. Plans, and even first measurements, are currently underway at the Jinping Underground Laboratory for Nuclear Astrophysics (JUNA) [66,115], Dresden Felsenkeller [15], and the Lab-

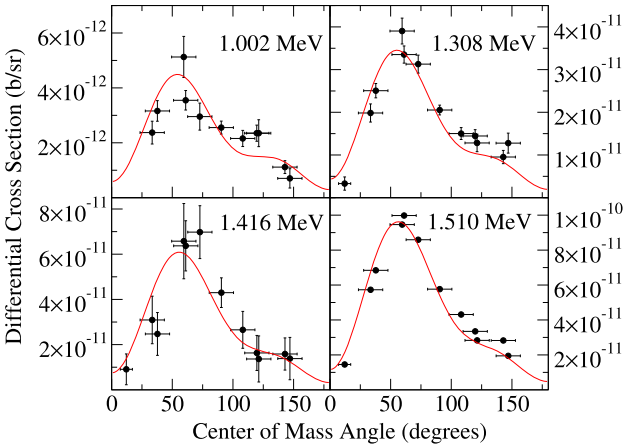

Fig. 13 Differential cross sections, at their associated center of mass energies, from Plag et al. [86] compared to the *R*-matrix fitting of deBoer et al. [36], but were not included in the fit

oratory for Underground Nuclear Astrophysics - Mega Volt (LUNA-MV) [43,87] facilities [6].

Some of the most impactful measurements in recent years were made using recoil separators [68,97,98]. In particular, through γ-ray coincidence, they have been able to pick out individual transitions with unsurpassed levels of precision. New measurements are also underway at the European Recoil Separator for Nuclear Astrophysics (ERNA), with the goal of expanding previous measurements over an even wider range of energies [6].

Other more indirect methods are also under consideration. Measurements of the inverse reaction, $^{16}O(\gamma,\alpha)^{12}C$ have been made at HIγS (High Intensity γ-Ray Source) [102] and further measurements are planned both at HIγS and ELI-NP [6]. Friščić et al. [47], Holt and Filippone [53] and Holt et al. [54] have all performed calculations to estimate the sensitivity that such measurements could reach and the impact that they could have on better determining the low energy *S*-factor.

On the observational side, LIGO continues to rapidly accumulate new measurements of black hole mergers, steadily decreasing the uncertainty on the size of the pair instability black hole mass gap. At the same time, ever increasing computational capability brings 3D stellar simulation with in closer reach. While astrophysical model uncertainties still don't provide definitive methods for deducing the $^{12}C(\alpha,\gamma)^{16}O$ reaction rate, this idea becomes closer to reality every day.

Funding RJD and MW utilized resources from the Notre Dame Center for Research Computing and were supported by the National Science Foundation through Grant No. PHY-2310059 (University of Notre Dame Nuclear Science Laboratory). This work was supported in part by the National Science Foundation under Grant No. OISE-1927130 (IReNA). The work of CRB was supported in part by the U.S. Department of Energy, under Grants No. DE-FG02-88ER40387 and No. DE-NA0004065. The work of WPL is supported by the National Key R&D Program of China (Grant No. 2022YFA1602301) and the National Natural Science Foundation of China (Grants No. 12435010, No. 11490560).

Data Availability Statement This manuscript has associated data in a data repository. [Author's comment: The datasets generated during and/or analysed during the current study are available in the EXFOR repository (https://www-nds.iaea.org/exfor/).]

Code Availability Statement This manuscript has associated code/software in a data repository. [Author's comment: This manuscript used the AZURE2 code for R-matrix calculations. The code is open source and is available at azure.nd.edu.]

References

1. B.P. Abbott, R. Abbott, T.D. Abbott, S. Abraham, F. Acernese et al., GWTC-1: a gravitational-wave transient catalog of compact binary mergers observed by LIGO and Virgo during the first and second observing runs. Phys. Rev. X **9**, 031040 (2019). https://doi.org/10.1103/PhysRevX.9.031040
2. R. Abbott, T.D. Abbott, S. Abraham, F. Acernese, K. Ackley et al., Properties and astrophysical implications of the 150 $M_\odot$ binary black hole merger GW190521. Astrophys. J. **900**(1), L13 (2020). https://doi.org/10.3847/2041-8213/aba493
3. R. Abbott, T.D. Abbott, F. Acernese, K. Ackley, C. Adams, N. Adhikari, R.X. Adhikari, V.B. Adya, C. Affeldt, D. Agarwal et al., GWTC-3: compact binary coalescences observed by LIGO and virgo during the second part of the third observing run. Phys. Rev. X **13**, 041039 (2023). https://doi.org/10.1103/PhysRevX.13.041039
4. S. Adhikari, C. Basu, P. Sugathan, A. Jhinghan, B.R. Behera, N. Saneesh, G. Kaur, M. Thakur, R. Mahajan, R. Dubey, A.K. Mitra, Breakup effects on alpha spectroscopic factors of ^{16}O. J. Phys. G Nucl. Phys. **44**(1), 015102 (2017). https://doi.org/10.1088/0954-3899/44/1/015102
5. S. Adhikari, C. Basu, The study of the reduced α-width and ANC of ^{16}O states through its sequential breakup. Phys. Lett. B **682**(2), 216–219 (2009). https://doi.org/10.1016/j.physletb.2009.11.009
6. M. Aliotta, R. Buompane, M. Couder, A. Couture, R.J. deBoer, A. Formicola, L. Gialanella, J. Glorius, G. Imbriani, M. Junker, C. Langer, A. Lennarz, Yu A. Litvinov, W. P. Liu, M. Lugaro, C. Matei, Z. Meisel, L. Piersanti, R. Reifarth, D. Robertson, A. Simon, O. Straniero, A. Tumino, M. Wiescher, Y. Xu. The status and future of direct nuclear reaction measurements for stellar burning. J. Phys. G Nucl. Phys. **49**(1), 010501 (2022). https://doi.org/10.1088/1361-6471/ac2b0f

7. S.-I. Ando, S matrices of elastic α -^{12}C scattering at low energies in effective field theory. Phys. Rev. C **107**(4), 045808 (2023). https://doi.org/10.1103/PhysRevC.107.045808
8. S.-I. Ando, Radiative decay of the subthreshold 1_1^- and 2_1^+ states of ^{16}O in cluster effective field theory. Phys. Rev. C **109**(1), 015801 (2024). https://doi.org/10.1103/PhysRevC.109.015801
9. W. David Arnett, Explosive nucleosynthesis in stars. ARA&A **11**, 73 (1973). https://doi.org/10.1146/annurev.aa.11.090173.000445
10. M. Assunção, M. Fey, A. Lefebvre-Schuhl, J. Kiener, V. Tatischeff, J.W. Hammer, C. Beck, C. Boukari-Pelissie, A. Coc, J.J. Correia, S. Courtin, F. Fleurot, E. Galanopoulos, C. Grama, F. Haas, F. Hammache, F. Hannachi, S. Harissopulos, A. Korichi, R. Kunz, D. Ledu, A. Lopez-Martens, D. Malcherek, R. Meunier, T. Paradellis, M. Rousseau, N. Rowley, G. Staudt, S. Szilner, J.P. Thibaud, J.L. Weil, $E1$ and $E2$ S factors of ^{12}C(α,γ_0)^{16}O from γ-ray angular distributions with a 4π-detector array. Phys. Rev. C **73**(5), 055801 (2006). https://doi.org/10.1103/PhysRevC.73.055801
11. M.L. Avila, G.V. Rogachev, E. Koshchiy, L.T. Baby, J. Belarge, K.W. Kemper, A.N. Kuchera, A.M. Mukhamedzhanov, D. Santiago-Gonzalez, E. Uberseder, Constraining the 6.05 MeV 0^+ and 6.13 MeV 3^- cascade transitions in the ^{12}C(α, γ)^{16}O reaction using the asymptotic normalization coefficients. Phys. Rev. Lett. **114**(7), 071101 (2015). https://doi.org/10.1103/PhysRevLett.114.071101
12. R.E. Azuma, E. Uberseder, E.C. Simpson, C.R. Brune, H. Costantini, R.J. de Boer, J. Görres, M. Heil, P.J. Leblanc, C. Ugalde, M. Wiescher, AZURE: an R-matrix code for nuclear astrophysics. Phys. Rev. C **81**(4), 045805 (2010). https://doi.org/10.1103/PhysRevC.81.045805
13. E.J. Baxter, D. Croon, S.D. McDermott, J. Sakstein, Find the gap: black hole population analysis with an astrophysically motivated mass function. Astrophys. J. Lett. **916**(2), L16 (2021). https://doi.org/10.3847/2041-8213/ac11fc**(ISSN 2041-8205, 2041-8213)**
14. A. Belhout, S. Ouichaoui, H. Beaumevieille, A. Boughrara, S. Fortier, J. Kiener, J.M. Maison, S.K. Mehdi, L. Rosier, J.P. Thibaud, A. Trabelsi, J. Vernotte, Measurement and DWBA analysis of the ^{12}C(^{6}Li,d)^{16}O α-transfer reaction cross sections at 48.2 MeV. R-matrix analysis of ^{12}C(α, γ)^{16}O direct capture reaction data. Nucl. Phys. A **793**(1), 178–211 (2007). https://doi.org/10.1016/j.nuclphysa.2007.06.008
15. D. Bemmerer, T.E. Cowan, M. Grieger, S. Hammer, T. Hensel, A.R. Junghans, M. Koppitz, F. Ludwig, S.E. Müller, B. Rimarzig, S. Reinicke, R. Schwengner, K. Stöckel, T. Szücs, M.P. Takács, S. Turkat, A. Wagner, L. Wagner, K. Zuber, Felsenkeller 5 MV underground accelerator: towards the holy grail of nuclear astrophysics ^{12}C(α, γ)^{16}O. In *European Physical Journal Web of Conferences, Volume 178 of European Physical Journal Web of Conferences* (2018), p. 01008. https://doi.org/10.1051/epjconf/201817801008
16. H.A. Bethe, C. Longmire, The effective range of nuclear forces II. Photo-disintegration of the deuteron. Phys. Rev. **77**(5), 647–654 (1950). https://doi.org/10.1103/PhysRev.77.647
17. A. Bischoff-Kim, A comparison of best fits obtained in white dwarf asteroseismology using the WDEC and the LPCODE. ApJ **974**(2), 183 (2024). https://doi.org/10.3847/1538-4357/ad701f
18. L.D. Blokhintsev, V.I. Kukulin, A.A. Sakharuk, D.A. Savin, E.V. Kuznetsova, Determination of the $^6\alpha$+d vertex constant (asymptotic coefficient) from the ^{4}He+d phase-shift analysis. Phys. Rev. C **48**(5), 2390–2394 (1993). https://doi.org/10.1103/PhysRevC.48.2390
19. L.D. Blokhintsev, A.S. Kadyrov, A.M. Mukhamedzhanov, D.A. Savin, Extrapolation of scattering data to the negative-energy region. II. Applicability of effective range functions within an exactly solvable model. Phys. Rev. C **97**(2), 024602 (2018). https://doi.org/10.1103/PhysRevC.97.024602
20. L. D. Blokhintsev, A.S. Kadyrov, A.M. Mukhamedzhanov, D.A. Savin, Determination of asymptotic normalization coefficients for the channel ^{16}O$\rightarrow$ α+^{12}C. I. Excited state ^{16}O (0^+;6.05 MeV). Eur. Phys. J. A **58**(12), 257 (2022). https://doi.org/10.1140/epja/s10050-022-00909-1
21. L.D. Blokhintsev, A.S. Kadyrov, A.M. Mukhamedzhanov, D.A. Savin, Determination of asymptotic normalization coefficients for the channel ^{16}O$\rightarrow$ α+^{12}C. II. Excited states ^{16}O(3^-, 2^+, 1^-). Eur. Phys. J. A **59**(7), 162 (2023). https://doi.org/10.1140/epja/s10050-023-01079-4
22. G. Bono, F. Caputo, S. Cassisi, M. Marconi, L. Piersanti, A. Tornambè, Intermediate-mass star models with different helium and metal contents. ApJ **543**(2), 955–971 (2000). https://doi.org/10.1086/317156
23. G.E. Brown, A. Heger, N. Langer, C.H. Lee, S. Wellstein, H.A. Bethe, Formation of high mass X-ray black hole binaries. New A **6**(7), 457–470 (2001). https://doi.org/10.1016/S1384-1076(01)00077-X
24. C.R. Brune, Alternative parametrization of R-matrix theory. Phys. Rev. C **66**(4), 044611 (2002). https://doi.org/10.1103/PhysRevC.66.044611
25. C.R. Brune, W.H. Geist, R.W. Kavanagh, K.D. Veal, Sub-Coulomb α transfers on ^{12}C and the ^{12}C(α, γ)^{16}O S factor. Phys. Rev. Lett. **83**(20), 4025–4028 (1999). https://doi.org/10.1103/PhysRevLett.83.4025
26. W.M. Brunish, S.A. Becker, Evolution of cepheids. I. The effects of an enhanced ^{12}C(α, γ)^{16}O rate. ApJ **351**, 258 (1990). https://doi.org/10.1086/168460
27. F. Caputo, V. Castellani, A. Chieffi, L. Pulone, A. Tornambe Jr., The "Red Giant Clock" as an indicator for the efficiency of central mixing in horizontal-branch stars. ApJ **340**, 241 (1989). https://doi.org/10.1086/167387
28. V. Castellani, A. Chieffi, A. Tornambe, L. Pulone, Helium-burning evolutionary phases in population II stars. I Breathing pulses in horizontal branch stars. ApJ **296**, 204–212 (1985). https://doi.org/10.1086/163437
29. M.T. Chidester, E. Farag, F.X. Timmes, On trapped modes in variable white dwarfs as probes of the ^{12}C(α, γ)^{16}O reaction rate. ApJ **935**(1), 21 (2022). https://doi.org/10.3847/1538-4357/ac7ec3
30. M.T. Chidester, F.X. Timmes, E. Farag, Seismic signatures of the ^{12}C(α, γ)^{16}O reaction rate in white dwarf models with overshooting. ApJ **954**(1), 51 (2023). https://doi.org/10.3847/1538-4357/ace620
31. A. Chieffi, M. Limongi, Pre-supernova evolution of rotating solar metallicity stars in the mass range 13–120 M $_\odot$ and their explosive yields. ApJ **764**(1), 21 (2013). https://doi.org/10.1088/0004-637X/764/1/21
32. A. Chieffi, M. Limongi, The presupernova core mass-radius relation of massive stars: understanding its formation and evolution. ApJ **890**(1), 43 (2020). https://doi.org/10.3847/1538-4357/ab6739
33. G.F. Ciani, L. Csedreki, D. Rapagnani, M. Aliotta, J. Balibrea-Correa, F. Barile, D. Bemmerer, A. Best, A. Boeltzig, C. Broggini, C.G. Bruno, A. Caciolli, F. Cavanna, T. Chillery, P. Colombetti, P. Corvisiero, S. Cristallo, T. Davinson, R. Depalo, A. Di Leva, Z. Elekes, F. Ferraro, E. Fiore, A. Formicola, Zs. Fülöp, G. Gervino, A. Guglielmetti, C. Gustavino, Gy. Gyürky, G. Imbriani, M. Junker, M. Lugaro, P. Marigo, E. Masha, R. Menegazzo, V. Mossa, F. R. Pantaleo, V. Paticchio, R. Perrino, D. Piatti, P. Prati, L. Schiavulli, K. Stöckel, O. Straniero, T. Szücs, M. P. Takács, F. Terrasi, D. Vescovi, S. Zavatarelli, LUNA Collaboration, Direct measurement of the ^{13}C(α,n)^{16}O cross section into the s-process Gamow peak. Phys. Rev. Lett. **127**(15), 152701 (2021). https://doi.org/10.1103/PhysRevLett.127.152701
34. T. Constantino, S.W. Campbell, J. Christensen-Dalsgaard, J.C. Lattanzio, D. Stello, The treatment of mixing in core helium

burning models—I. Implications for asteroseismology. MNRAS **452**(1), 123–145 (2015). https://doi.org/10.1093/mnras/stv1264
35. T. Constantino, S.W. Campbell, J.C. Lattanzio, A. van Duijneveldt, The treatment of mixing in core helium burning models—II. Constraints from cluster star counts. MNRAS **456**(4), 3866–3885 (2016). https://doi.org/10.1093/mnras/stv2939
36. R.J. deBoer, J. Görres, M. Wiescher, R.E. Azuma, A. Best, C.R. Brune, C.E. Fields, S. Jones, M. Pignatari, D. Sayre, K. Smith, F.X. Timmes, E. Uberseder, The $^{12}C(\alpha,\gamma)^{16}O$ reaction and its implications for stellar helium burning. Rev. Mod. Phys. **89**(3), 035007 (2017). https://doi.org/10.1103/RevModPhys.89.035007
37. P. Descouvemont, D. Baye, The *R*-matrix theory. Rep. Prog. Phys. **73**(3), 036301 (2010). https://doi.org/10.1088/0034-4885/73/3/036301
38. H.W. Drotleff, A. Denker, H. Knee, M. Soine, G. Wolf, J.W. Hammer, U. Greife, C. Rolfs, H.P. Trautvetter, Reaction rates of the *s*-process neutron sources $^{22}Ne(\alpha,n)^{25}Mg$ and $^{13}C(\alpha,n)^{16}O$. ApJ **414**, 735 (1993). https://doi.org/10.1086/173119
39. P. Ducru, V. Sobes, Definite complete invariant parametrization of R-matrix theory. Phys. Rev. C **105**(2), 024601 (2022). https://doi.org/10.1103/PhysRevC.105.024601
40. P. Dyer, C.A. Barnes, The $^{12}C(\alpha,\gamma)^{16}O$ reaction and stellar helium burning. Nucl. Phys. A **233**(2), 495–520 (1974). https://doi.org/10.1016/0375-9474(74)90470-9
41. R. Farmer, M. Renzo, S.E. de Mink, P. Marchant, S. Justham, Mind the gap: the location of the lower edge of the pair-instability supernova black hole mass gap. ApJ **887**(1), 53 (2019). https://doi.org/10.3847/1538-4357/ab518b
42. R. Farmer, M. Renzo, S.E. de Mink, M. Fishbach, S. Justham, Constraints from gravitational-wave detections of binary black hole mergers on the $^{12}C(\alpha,\gamma)^{16}O$ rate. ApJ **902**(2), L36 (2020). https://doi.org/10.3847/2041-8213/abbadd
43. F. Ferraro, G.F. Ciani, A. Boeltzig, F. Cavanna, S. Zavatarelli, The study of key reactions shaping the post-main sequence evolution of massive stars in underground facilities. Front. Astron. Space Sci. **7**, 119 (2021). https://doi.org/10.3389/fspas.2020.617946
44. M. Fey. Im Brennpunkt der Nuklearen Astrophysik: Die Reaktion $^{12}C(\alpha,\gamma)^{16}O$. PhD thesis, Universität Stuttgart (2004)
45. C.E. Fields, R. Farmer, I. Petermann, C. Iliadis, F.X. Timmes, Properties of carbon-oxygen white dwarfs from Monte Carlo stellar models. ApJ **823**(1), 46 (2016). https://doi.org/10.3847/0004-637X/823/1/46
46. G. Fontaine, P. Brassard, Can white dwarf asteroseismology really constrain the $^{12}C(\alpha,\gamma)^{16}O$ reaction rate? ApJ **581**(1), L33–L37 (2002). https://doi.org/10.1086/345787
47. I. Friščić, T.W. Donnelly, R.G. Milner, New approach to determining radiative capture reaction rates at astrophysical energies. Phys. Rev. C **100**(2), 025804 (2019). https://doi.org/10.1103/PhysRevC.100.025804
48. T. Fukui, Y. Kanada-En'yo, K. Ogata, T. Suhara, Y. Taniguchi, Investigation of spatial manifestation of α clusters in ^{16}O via α-transfer reactions. Nucl. Phys. A **983**, 38–52 (2019). https://doi.org/10.1016/j.nuclphysa.2018.12.024
49. B. Gao, T.Y. Jiao, Y.T. Li, H. Chen, W.P. Lin, Z. An, L.H. Ru, Z.C. Zhang, X.D. Tang, X.Y. Wang, N.T. Zhang, X. Fang, D.H. Xie, Y.H. Fan, L. Ma, X. Zhang, F. Bai, P. Wang, Y.X. Fan, G. Liu, H.X. Huang, Q. Wu, Y.B. Zhu, J.L. Chai, J.Q. Li, L.T. Sun, S. Wang, J.W. Cai, Y.Z. Li, J. Su, H. Zhang, Z.H. Li, Y.J. Li, E.T. Li, C. Chen, Y.P. Shen, G. Lian, B. Guo, X.Y. Li, L.Y. Zhang, J.J. He, Y.D. Sheng, Y.J. Chen, L.H. Wang, L. Zhang, F.Q. Cao, W. Nan, W.K. Nan, G.X. Li, N. Song, B.Q. Cui, L.H. Chen, R.G. Ma, Z.C. Zhang, S.Q. Yan, J.H. Liao, Y.B. Wang, S. Zeng, D. Nan, Q.W. Fan, N.C. Qi, W.L. Sun, X.Y. Guo, P. Zhang, Y.H. Chen, Y. Zhou, J.F. Zhou, J.R. He, C.S. Shang, M.C. Li, S. Kubono, W.P. Liu, R.J. deBoer, M. Wiescher, M. Pignatari, JUNA Collaboration, Deep underground laboratory measurement of $^{13}C(\alpha,n)^{16}O$ in the Gamow windows of the *s* and *i* processes. Phys. Rev. Lett. **129**(13), 132701 (2022). https://doi.org/10.1103/PhysRevLett.129.132701
50. L. Gialanella, D. Rogalla, F. Strieder, S. Theis, G. Gyürki, C. Agodi, R. Alba, M. Aliotta, L. Campajola, A. Del Zoppo, A. D'Onofrio, P. Figuera, U. Greife, G. Imbriani, A. Ordine, V. Roca, C. Rolfs, M. Romano, C. Sabbarese, P. Sapienza, F. Schümann, E. Somorjai, F. Terrasi, H.P. Trautvetter, The E1 capture amplitude in $^{12}C(\alpha,\gamma_0)^{16}O$. Eur. Phys. J. A **11**(3), 357–370 (2001). https://doi.org/10.1007/s100500170075
51. C. Hebborn, G. Hupin, K. Kravvaris, S. Quaglioni, P. Navrátil, P. Gysbers, Ab initio prediction of the $^{4}He(d,\gamma)^{6}Li$ big bang radiative capture. Phys. Rev. Lett. **129**(4), 042503 (2022). https://doi.org/10.1103/PhysRevLett.129.042503
52. C. Hebborn, M.L. Avila, K. Kravvaris, G. Potel, S. Quaglioni, Impact of the ^{6}Li asymptotic normalization constant onto α -induced reactions of astrophysical interest. Phys. Rev. C **109**(6), L061601 (2024). https://doi.org/10.1103/PhysRevC.109.L061601
53. R.J. Holt, B.W. Filippone, Impact of $^{16}O(e, e'\alpha)^{12}C$ measurements on the $^{12}C(\alpha,\gamma)^{16}O$ astrophysical reaction rate. Phys. Rev. C **100**(6), 065802 (2019). https://doi.org/10.1103/PhysRevC.100.065802
54. R.J. Holt, B.W. Filippone, S.C. Pieper, Impact of $^{16}O(\gamma,\alpha)^{12}C$ measurements on the $^{12}C(\alpha,\gamma)^{16}O$ astrophysical reaction rate. Phys. Rev. C **99**(5), 055802 (2019). https://doi.org/10.1103/PhysRevC.99.055802
55. F. Hoyle. On nuclear reactions occuring in very hot STARS. I. The synthesis of elements from carbon to nickel. ApJS **1**, 121 (1954). https://doi.org/10.1086/190005
56. Icko Jr. Iben. Cepheids, Presupernovae, the $^{12}C(\alpha,\gamma)^{16}0$ reaction. ApJ **178**, 433–440 (1972). https://doi.org/10.1086/151802
57. G. Imbriani, M. Limongi, L. Gialanella, F. Terrasi, O. Straniero, A. Chieffi, The $^{12}C(\alpha,\gamma)^{16}O$ reaction rate and the evolution of stars in the mass range $0.8 \leq M/M_{solar} \leq 25$. ApJ **558**(2), 903–915 (2001). https://doi.org/10.1086/322288
58. K.U. Kettner, H.W. Becker, L. Buchmann, J. Görres, H. Kräwinkel, C. Rolfs, P. Schmalbrock, H.P. Trautvetter, A. Vlieks, The $^{4}He(^{12}C,\gamma)^{16}O$ reaction at stellar energies. Zeitschrift fur Physik A Hadrons and Nuclei **308**(1), 73–94 (1982). https://doi.org/10.1007/BF01415851
59. K. Kravvaris, S. Quaglioni, G. Hupin, P. Navrátil, Ab initio framework for nuclear scattering and reactions induced by light projectiles. Phys. Lett. B **856**, 138930 (2024). https://doi.org/10.1016/j.physletb.2024.138930
60. R.M. Kremer, C.A. Barnes, K.H. Chang, H.C. Evans, B.W. Filippone, Coincidence measurement of the $^{12}C(\alpha,\gamma)^{16}O$ cross section at low energies. Phys. Rev. Lett. **60**, 1475–1478 (1988). https://doi.org/10.1103/PhysRevLett.60.1475
61. R. Kunz, M. Jaeger, A. Mayer, J.W. Hammer, G. Staudt, S. Harissopulos, T. Paradellis, $^{12}C(\alpha,\gamma)^{16}O$: the key reaction in stellar nucleosynthesis. Phys. Rev. Lett. **86**(15), 3244–3247 (2001). https://doi.org/10.1103/PhysRevLett.86.3244
62. R. Kunz, M. Fey, M. Jaeger, A. Mayer, J.W. Hammer, G. Staudt, S. Harissopulos, T. Paradellis, Astrophysical reaction rate of $^{12}C(\alpha,\gamma)^{16}O$. ApJ **567**(1), 643–650 (2002). https://doi.org/10.1086/338384
63. A.M. Lane, R.G. Thomas, *R*-matrix theory of nuclear reactions. Rev. Mod. Phys. **30**(2), 257–353 (1958). https://doi.org/10.1103/RevModPhys.30.257
64. K.D. Launey, A. Mercenne, T. Dytrych, Nuclear dynamics and reactions in the ab initio symmetry-adapted framework. Annu. Rev. Nucl. Part. Sci. **71**, 253–277 (2021). https://doi.org/10.1146/annurev-nucl-102419-033316
65. M. Limongi, A. Chieffi, Presupernova evolution and explosive nucleosynthesis of rotating massive stars in the metallicity range

-3 ≤ ≤ 0. ApJS **237**(1), 13 (2018). https://doi.org/10.3847/1538-4365/aacb24
66. W. Liu, Z. Li, J. He, X. Tang, G. Lian, J. Su, Y. Shen, Z. An, F. Chao, J. Chang, L. Chen, H. Chen, X. Chen, Y. Chen, Z. Chen, J. Cheng, B. Cui, X. Fang, C. Fu, L. Gan, B. Guo, Z. Han, X. Guo, G. He, J. He, A. Heger, S. Hou, H. Huang, N. Huang, B. Jia, L. Jiang, S. Kubono, J. Li, M. Li, K. Li, E. Li, T. Li, Y. Li, M. Lugaro, X. Luo, H. Ma, S. Ma, D. Mei, W. Nan, W. Nan, N. Qi, Y. Qian, J. Qin, J. Ren, C. Shang, L. Sun, W. Sun, W. Tan, I. Tanihata, S. Wang, P. Wang, Y. Wang, Q. Wu, S. Xu, Y. Yang, X. Yu, Q. Yue, S. Zeng, L. Zhang, H. Zhang, H. Zhang, L. Zhang, N. Zhang, P. Zhang, Q. Zhang, T. Zhang, X. Zhang, X. Zhang, W. Zhao, J. Zhou, Y. Zhou. Commissioning of Underground Nuclear Astrophysics Experiment JUNA in China. In *European Physical Journal Web of Conferences, Volume 260 of European Physical Journal Web of Conferences* (2022), p. 08001. https://doi.org/10.1051/epjconf/202226008001
67. H. Makii, Y. Nagai, T. Shima, M. Segawa, K. Mishima, H. Ueda, M. Igashira, T. Ohsaki, $E1$ and $E2$ cross sections of the $^{12}C(\alpha,\gamma_0)^{16}O$ reaction using pulsed α beams. Phys. Rev. C **80**(6), 065802 (2009). https://doi.org/10.1103/PhysRevC.80.065802
68. C. Matei, L. Buchmann, W.R. Hannes, D.A. Hutcheon, C. Ruiz, C.R. Brune, J. Caggiano, A.A. Chen, J. D'Auria, A. Laird, M. Lamey, Zh. Li, Wp. Liu, A. Olin, D. Ottewell, J. Pearson, G. Ruprecht, M. Trinczek, C. Vockenhuber, C. Wrede, Measurement of the cascade transition via the first excited state of O16 in the $^{12}C(\alpha,\gamma)^{16}O$ reaction, and its S factor in stellar helium burning. Phys. Rev. Lett. **97**(24), 242503 (2006). https://doi.org/10.1103/PhysRevLett.97.242503
69. A.K. Mehta, A. Buonanno, J. Gair, M.C. Miller, E. Farag, R.J. deBoer, M. Wiescher, F.X. Timmes, Observing intermediate-mass black holes and the upper stellar-mass gap with LIGO and Virgo. ApJ **924**(1), 39 (2022). https://doi.org/10.3847/1538-4357/ac3130
70. T.S. Metcalfe, M. Salaris, D.E. Winget, Measuring $^{12}C(\alpha,\gamma)^{16}O$ from white dwarf asteroseismology. ApJ **573**(2), 803–811 (2002). https://doi.org/10.1086/340796
71. T.S. Metcalfe, White dwarf asteroseismology and the $^{12}C(\alpha,\gamma)^{16}O$ rate. ApJ **587**(1), L43–L46 (2003). https://doi.org/10.1086/375044
72. A.K. Mondal, C. Basu, S. Adhikari, C. Bhattacharya, T.K. Rana, S. Kundu, S. Manna, R. Pandey, P. Roy, A. Sen, J.K. Meena, A.K. Saha, J.K. Sahoo, D. Basak, T. Bar, H. Pai, A. Bisoi, A.K. Mitra, P. Biswas, $^{12}C(^{20}Ne,^{16}O)^{16}O$ α-transfer reaction and astrophysical S-factors at 300 keV. Int. J. Mod. Phys. E **30**(5), 2150039-8 (2021). https://doi.org/10.1142/S0218301321500397
73. M.C. Morais, R. Lichtenthäler, α-Spectroscopic factor of $^{16}O_{gs}$ from the $^{12}C(^{16}O,^{12}C)^{16}O$ reaction. Nucl. Phys. A **857**(1), 1–8 (2011). https://doi.org/10.1016/j.nuclphysa.2011.03.005
74. J. Moscoso, R.S. de Souza, A. Coc, C. Iliadis, Bayesian estimation of the $d(p,\gamma)^3$He thermonuclear reaction rate. ApJ **923**(1), 49 (2021). https://doi.org/10.3847/1538-4357/ac1db0
75. A.M. Mukhamedzhanov, C.A. Gagliardi, R.E. Tribble, Asymptotic normalization coefficients, spectroscopic factors, and direct radiative capture rates. Phys. Rev. C **63**(2), 024612 (2001). https://doi.org/10.1103/PhysRevC.63.024612
76. A.M. Mukhamedzhanov, R.J. deBoer, B.F. Irgaziev, L.D. Blokhintsev, A.S. Kadyrov, D.A. Savin, Asymptotic normalization coefficients for $\alpha + ^{12}$ C synthesis and the S-factor for $^{12}C(\alpha,\gamma)^{16}O$ radiative capture. Phys. Rev. C **110**(5), 055803 (2024). https://doi.org/10.1103/PhysRevC.110.055803
77. W. Nan, Y.P. Shen, B. Guo, Z.H. Li, Y.J. Li, D.Y. Pang, J. Su, S.Q. Yan, Q.W. Fan, J.C. Liu, C. Chen, X.Y. Li, G. Lian, T.L. Ma, W.K. Nan, Y.B. Wang, S. Zeng, H. Zhang, W.P. Liu, New determination of the astrophysical S_{E1} factor of the $^{12}C(\alpha,\gamma)^{16}O$ reaction via the $^{12}C(^{11}B,^{7}Li)^{16}O$ transfer reaction. Phys. Rev. C **109**(4), 045808 (2024). https://doi.org/10.1103/PhysRevC.109.045808
78. P. Navrátil, S, Quaglioni, in *Ab Initio Nuclear Reaction Theory with Applications to Astrophysics* (Springer Nature Singapore, Singapore, 2020), pp. 1–46. https://doi.org/10.1007/978-981-15-8818-1_7-1**(ISBN 978-981-15-8818-1)**
79. T. Nugis, H. Lamers, Mass-loss rates of Wolf-Rayet stars as a function of stellar parameters. A&A **360**, 227–244 (2000)
80. D. Odell, C.R. Brune, D.R. Phillips, How Bayesian methods can improve R-matrix analyses of data: the example of the dt reaction. Phys. Rev. C **105**(1), 014625 (2022). https://doi.org/10.1103/PhysRevC.105.014625
81. D. Odell, C.R. Brune, D.R. Phillips, R.J. deBoer, S.N. Paneru, Performing Bayesian analyses with AZURE2 using BRICK: an application to the ^{7}Be system. Front. Phys. **10**, 888476 (2022b). https://doi.org/10.3389/fphy.2022.888476
82. Yu. V. Orlov, B.F. Irgaziev, J.-U. Nabi. Algorithm for calculations of asymptotic nuclear coefficients using phase-shift data for charged-particle scattering. Phys. Rev. C **96**(2), 025809 (2017). https://doi.org/10.1103/PhysRevC.96.025809
83. J. Ouellet, H.C. Evans, H.W. Lee, J.R. Leslie, J.D. MacArthur, W. McLatchie, H.B. Mak, P. Skensved, J.L. Whitton, X. Zhao, T.K. Alexander, $^{12}C(\alpha,\gamma)^{16}O$ cross sections at stellar energies. Phys. Rev. Lett. **69**(13), 1896–1899 (1992). https://doi.org/10.1103/PhysRevLett.69.1896
84. N. Oulebsir, F. Hammache, P. Roussel, M.G. Pellegriti, L. Audouin, D. Beaumel, A. Bouda, P. Descouvemont, S. Fortier, L. Gaudefroy, J. Kiener, A. Lefebvre-Schuhl, V. Tatischeff, Indirect study of the $^{12}C(\alpha,\gamma)^{16}O$ reaction via the $^{12}C(^7Li, t)^{16}O$ transfer reaction. Phys. Rev. C **85**(3), 035804 (2012). https://doi.org/10.1103/PhysRevC.85.035804
85. T.-S. Park, R-matrix theory with level-dependent boundary condition parameters. Phys. Rev. C **104**(6), 064612 (2021). https://doi.org/10.1103/PhysRevC.104.064612
86. R. Plag, R. Reifarth, M. Heil, F. Käppeler, G. Rupp, F. Voss, K. Wisshak, $^{12}C(\alpha,\gamma)^{16}O$ studied with the Karlsruhe 4π BaF_2 detector. Phys. Rev. C **86**(1), 015805 (2012). https://doi.org/10.1103/PhysRevC.86.015805
87. P. Prati, LUNA Collaboration, The LUNA-MV facility at Gran Sasso. In *Journal of Physics Conference Series, Volume 1342 of Journal of Physics Conference Series*. IOP (2020), p. 012088. https://doi.org/10.1088/1742-6596/1342/1/012088
88. O.L. Ramírez Suárez, J.M. Sparenberg, Phase-shift parametrization and extraction of asymptotic normalization constants from elastic-scattering data. Phys. Rev. C **96**(3), 034601 (2017). https://doi.org/10.1103/PhysRevC.96.034601
89. A. Redder, H.W. Becker, C. Rolfs, H.P. Trautvetter, T.R. Donoghue, T.C. Rinckel, J.W. Hammer, K. Langanke, The $^{12}C(\alpha,\gamma)^{16}O$ cross section at stellar energies. Nucl. Phys. A **462**(2), 385–412 (1987). https://doi.org/10.1016/0375-9474(87)90555-0
90. A. Renzini, Why stars inflate to and deflate from red giant dimensions—II. Replies to critics. MNRAS **521**(1), 524–529 (2023). https://doi.org/10.1093/mnras/stad159
91. M. Renzo, N. Smith, Pair-instability evolution and explosions in massive stars. arXiv:2407.16113 (2024). https://doi.org/10.48550/arXiv.2407.16113
92. L. Roberti, M. Limongi, A. Chieffi, Presupernova evolution and explosive nucleosynthesis of rotating massive stars. II. The supersolar models at = 0.3. ApJS **272**(1), 15 (2024). https://doi.org/10.3847/1538-4365/ad391d
93. G. Roters, C. Rolfs, F. Strieder, H.P. Trautvetter, The E1 and E2 capture amplitudes in $^{12}C(\alpha,\gamma_0)^{16}O$. Eur. Phys. J. A **6**(4), 451–461 (1999). https://doi.org/10.1007/s100500050369
94. M. Salaris, I. Domínguez, E. García-Berro, M. Hernanz, J. Isern, R. Mochkovitch, The cooling of CO white dwarfs: influence of

the internal chemical distribution. ApJ **486**(1), 413–419 (1997). https://doi.org/10.1086/304483
95. R. Satchler, *Direct Nuclear Reactions* (Clarendon Press, Oxford, 1983)
96. D.B. Sayre, C.R. Brune, D.E. Carter, D.K. Jacobs, T.N. Massey, J.E. O'Donnell, E2 interference effects in the $^{12}C(\alpha,\gamma_0)^{16}O$ reaction. Phys. Rev. Lett. **109**(14), 142501 (2012). https://doi.org/10.1103/PhysRevLett.109.142501
97. D. Schürmann, A. Di Leva, L. Gialanella, D. Rogalla, F. Strieder, N. De Cesare, A. D'Onofrio, G. Imbriani, R. Kunz, C. Lubritto, A. Ordine, V. Roca, C. Rolfs, M. Romano, F. Schümann, F. Terrasi, H.P. Trautvetter, First direct measurement of the total cross-section of $^{12}C(\alpha,\gamma)^{16}O$. Eur. Phys. J. A **26**(2), 301–305 (2005). https://doi.org/10.1140/epja/i2005-10175-2
98. D. Schürmann, A. Di Leva, L. Gialanella, R. Kunz, F. Strieder, N. De Cesare, M. De Cesare, A. D'Onofrio, K. Fortak, G. Imbriani, D. Rogalla, M. Romano, F. Terrasi, Study of the 6.05 MeV cascade transition in $^{12}C(\alpha,\gamma)^{16}O$. Phys. Lett. B **703**(5), 557–561 (2011). https://doi.org/10.1016/j.physletb.2011.08.061
99. Y.P. Shen, B. Guo, Z.H. Li, Y.J. Li, D.Y. Pang, S. Adhikari, Z.D. An, J. Su, S.Q. Yan, X.C. Du, Q.W. Fan, L. Gan, Z.Y. Han, D.H. Li, E.T. Li, X.Y. Li, G. Lian, J.C. Liu, T.L. Ma, C.J. Pei, Y. Su, Y.B. Wang, S. Zeng, Y. Zhou, W.P. Liu, Astrophysical S_{E2} factor of the $^{12}C(\alpha,\gamma)^{16}O$ reaction through the $^{12}C(^{11}B,^{7}Li)^{16}O$ transfer reaction. Phys. Rev. C **99**(2), 025805 (2019). https://doi.org/10.1103/PhysRevC.99.025805
100. Y.P. Shen, B. Guo, R.J. deBoer, Z.H. Li, Y.J. Li, X.D. Tang, D.Y. Pang, S. Adhikari, C. Basu, J. Su, S. Q. Yan, Q.W. Fan, J.C. Liu, C. Chen, Z.Y. Han, X.Y. Li, G. Lian, T.L. Ma, W. Nan, W.K. Nan, Y.B. Wang, S. Zeng, H. Zhang, W.P. Liu, Constraining the external capture to the ^{16}O ground state and the $E2$ S factor of the $^{12}C(\alpha,\gamma)^{16}O$ reaction. Phys. Rev. Lett. **124**(16), 162701 (2020). https://doi.org/10.1103/PhysRevLett.124.162701
101. Y. Shen, B. Guo, R.J. deBoer, E. Li, Z. Li, Y. Li, X. Tang, D. Pang, S. Adhikari, C. Basu, J. Su, S. Yan, Q. Fan, J. Liu, C. Chen, Z. Han, X. Li, G. Lian, T. Ma, W. Nan, W. Nan, Y. Wang, S. Zeng, H. Zhang, W. Liu, New determination of the $^{12}C(\alpha,\gamma)^{16}O$ reaction rate and its impact on the black-hole mass gap. ApJ **945**(1), 41 (2023). https://doi.org/10.3847/1538-4357/acb7de
102. R. Smith, M. Gai, S.R. Stern, D.K. Schweitzer, M.W. Ahmed, Precision measurements on oxygen formation in stellar helium burning with gamma-ray beams and a time projection chamber. Nat. Commun. **12**, 5920 (2021). https://doi.org/10.1038/s41467-021-26179-x
103. R.J. Stancliffe, A. Chieffi, J.C. Lattanzio, R.P. Church, Why do low-mass stars become red giants? PASA **26**(3), 203–208 (2009). https://doi.org/10.1071/AS08060
104. O. Straniero, I. Domínguez, G. Imbriani, L. Piersanti, The chemical composition of white dwarfs as a test of convective efficiency during core helium burning. ApJ **583**(2), 878–884 (2003). https://doi.org/10.1086/345427
105. T. Sukhbold, S.E. Woosley, A. Heger, A high-resolution study of presupernova core structure. ApJ **860**(2), 93 (2018). https://doi.org/10.3847/1538-4357/aac2da
106. K. Takahashi, The low detection rate of pair-instability supernovae and the effect of the core carbon fraction. ApJ **863**(2), 153 (2018). https://doi.org/10.3847/1538-4357/aad2d2
107. T. Teichmann, On the interpretation of resonance levels and their widths in terms of the scattering length and the effective range. Phys. Rev. **83**(1), 141–145 (1951). https://doi.org/10.1103/PhysRev.83.141
108. I.J. Thomspon, F.M. Nunes, *Nuclear Reactions for Astrophysics* (Cambridge University Press, Cambridge, 2009)
109. P. Tischhauser, A. Couture, R. Detwiler, J. Görres, C. Ugalde, E. Stech, M. Wiescher, M. Heil, F. Käppeler, R.E. Azuma, L. Buchmann, Measurement of elastic C12+α scattering: details of the experiment, analysis, and discussion of phase shifts. Phys. Rev. C **79**(5), 055803 (2009). https://doi.org/10.1103/PhysRevC.79.055803
110. R.E. Tribble, C.A. Bertulani, M. La Cognata, A.M. Mukhamedzhanov, C. Spitaleri, Indirect techniques in nuclear astrophysics: a review. Rep. Prog. Phys. **77**(10), 106901 (2014). https://doi.org/10.1088/0034-4885/77/10/106901
111. C. Tur, A. Heger, S.M. Austin, On the sensitivity of massive star nucleosynthesis and evolution to solar abundances and to uncertainties in helium-burning reaction rates. ApJ **671**(1), 821–827 (2007). https://doi.org/10.1086/523095
112. C. Tur, A. Heger, S.M. Austin, Dependence of s-process nucleosynthesis in massive stars on triple-alpha and $^{12}C(\alpha,\gamma)^{16}O$ reaction rate uncertainties. ApJ **702**(2), 1068–1077 (2009). https://doi.org/10.1088/0004-637X/702/2/1068
113. C. Tur, A. Heger, S.M. Austin, Production of ^{26}Al, ^{44}Ti, and ^{60}Fe in core-collapse supernovae: sensitivity to the rates of the triple alpha and $^{12}C(\alpha,\gamma)^{16}O$ reactions. ApJ **718**(1), 357–367 (2010). https://doi.org/10.1088/0004-637X/718/1/357
114. H. Umeda, K. Nomoto, H. Yamaoka, S. Wanajo, Evolution of 3-9 M_{solar} stars for Z = 0.001-0.03 and metallicity effects on type Ia supernovae. ApJ **513**(2), 861–868 (1999). https://doi.org/10.1086/306887
115. L.H. Wang, Y.P. Shen, J. Su, X.Y. Li, W.Q. Yan, J.J. He, L.Y. Zhang, B. Liao, Y.F. Wu, Y.D. Sheng, Z.M. Li, Y.J. Chen, L.Y. Song, X.Z. Jiang, G. Lian, W. Nan, W.K. Nan, L. Zhang, F.Q. Cao, C. Chen, N. Song, H. Zhang, W.P. Liu, Development of irradiation-resistant enriched ^{12}C targets for astrophysical $^{12}C(\alpha,\gamma)^{16}O$ reaction measurements. Nucl. Instrum. Methods Phys. Res. B **512**, 49–53 (2022). https://doi.org/10.1016/j.nimb.2021.11.020
116. T.A. Weaver, S.E. Woosley, Nucleosynthesis in massive stars and the $^{12}C(\alpha,\gamma)^{16}O$ reaction rate. Phys. Rep. **227**(1–5), 65–96 (1993). https://doi.org/10.1016/0370-1573(93)90058-L
117. H.R. Weller, M.W. Ahmed, Y.K. Wu, Nuclear physics research at the high intensity gamma-ray source (HIγS). Nucl. Phys. News **25**(3), 19–24 (2015). https://doi.org/10.1080/10619127.2015.1035932
118. C. West, A. Heger, S.M. Austin, The impact of helium-burning reaction rates on massive star evolution and nucleosynthesis. ApJ **769**(1), 2 (2013). https://doi.org/10.1088/0004-637X/769/1/2
119. D. Wiarda, G. Arbanas, J.M. Brown, A.M. Holcomb, M.T. Pigni, J. McDonnel, C. Chapman, Modernization efforts for the R-Matrix code SAMMY. In *European Physical Journal Web of Conferences, Volume 284 of European Physical Journal Web of Conferences* (2023), p. 12005. https://doi.org/10.1051/epjconf/202328412005
120. S.E. Woosley, A. Heger, The pair-instability mass gap for black holes. Astrophys. J. Lett. **912**(2),L31 (2021). https://doi.org/10.3847/2041-8213/abf2c4**(ISSN 2041-8205, 2041-8213)**